Discussion

In a previous study (Misawa *et al.*, 2005), we identified the *PTGDR* and *PTGER2* genes as possible targets for DNA methylation in advanced types of NB. In the work presented here, we have demonstrated that expression of *PTGER2* was often silenced in NB cell lines through epigenetic mechanisms such as DNA methylation and

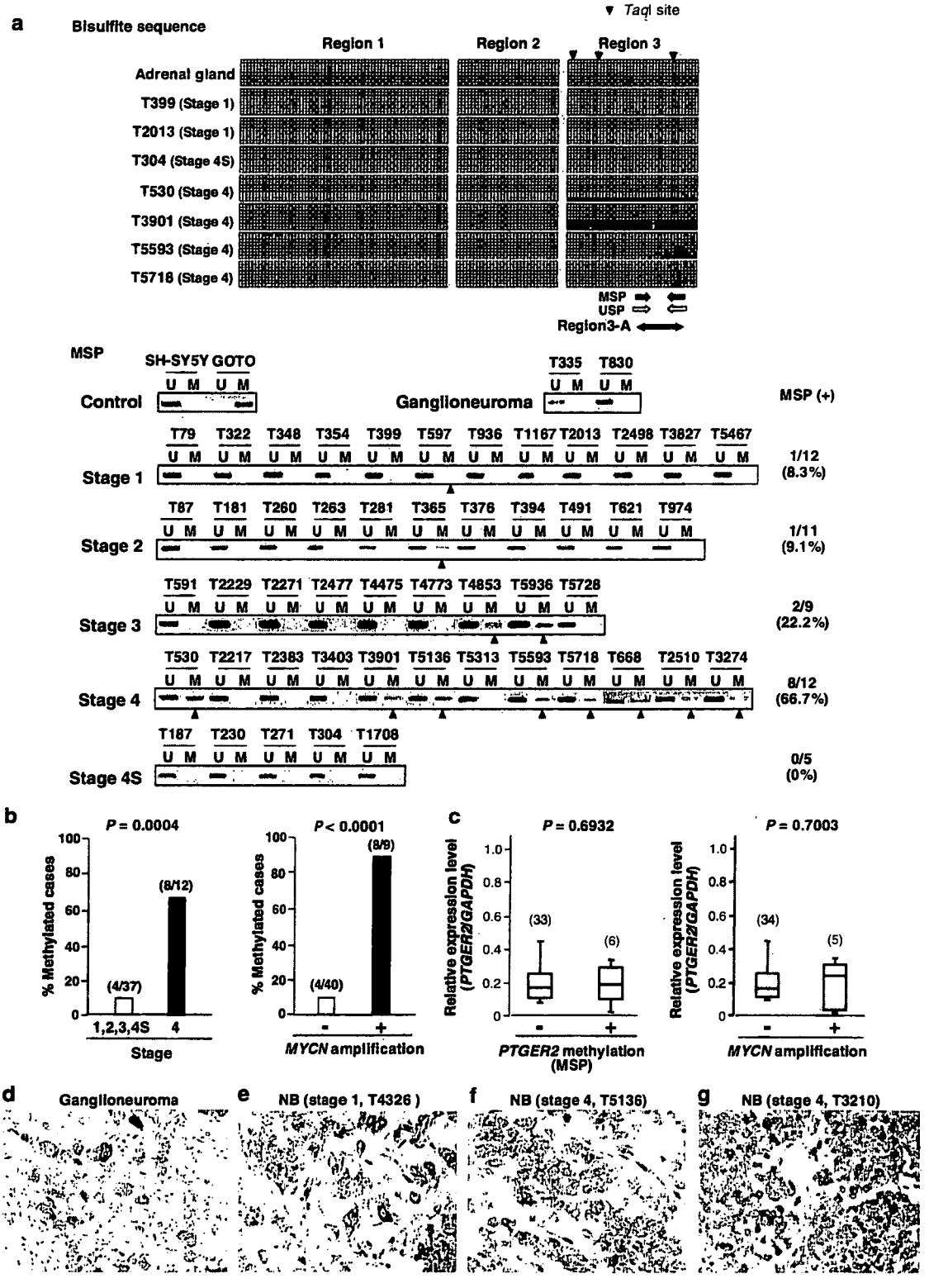

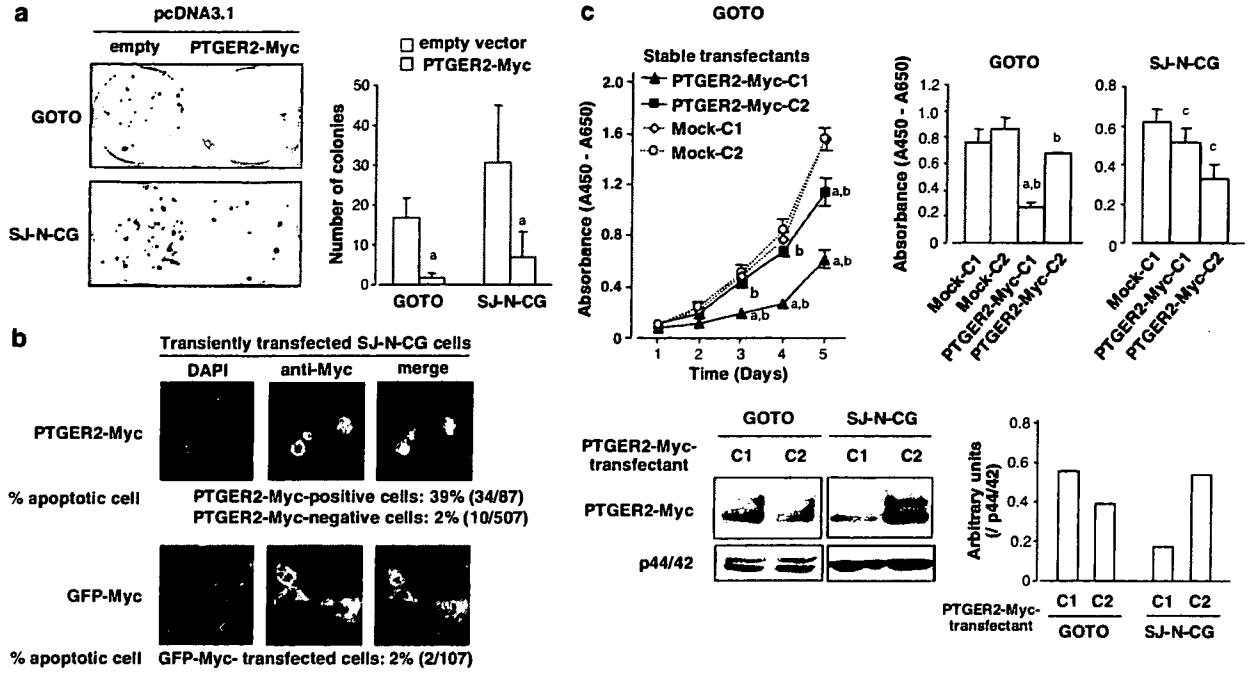

Figure 4 Effect of restoration of *PTGER2* expression on growth of NB cells. (**a**) Colony-formation assays using two NB cell lines without *PTGER2* expression (GOTO and SJ-N-CG). The cells were transiently transfected with a Myc-tagged construct containing *PTGER2* (pcDNA3.1-*PTGER2*-Myc), or empty vector (pcDNA3.1-empty) and selected for 2–3 weeks with appropriate concentrations of G418. Left: Two (SJ-N-CG) or three (GOTO) weeks after transfection and subsequent selection of drug-resistant colonies, the colonies formed by *PTGER2*-transfected cells were less numerous than those formed by empty vector-transfected cells. Right, Quantitative analysis of colony formation. Colonies larger than 2 mm were counted, and results are presented as means ± s.d. of representative of three separate experiments, each performed in triplicate. Statistical analysis used the Mann–Whitney *U*-test: (**a**) $P<0.05$ versus empty vector-transfected cells. (**b**) Fluorescent immunocytochemical analysis of SJ-N-CG cells transiently transfected with Myc-tagged *PTGER2* and stained with anti-Myc-tag antibody. Notably, cells with typical apoptotic changes, such as condensation or fragmentation of nuclear chromatin, were observed more frequently in PTGER2-Myc-positive NB cells compared with either PTGER2-Myc-negative cells or control GFP-Myc-transfected cells. (**c**) Effect of stable PTGER2 expression on the growth of GOTO and SJ-N-CG cells. Viability was determined by WST assay at the indicated times. The data presented are the means ± s.d. of three separate experiments. Statistical analysis used one-way ANOVA with subsequent Scheffé's tests: (**a**) PTGER2-transfected clone versus mock control clone C1 established from GOTO cells; (**b**) PTGER2-transfected clone versus mock control clone C2 established from GOTO cells; (**c**) PTGER2-transfected clone versus mock control clone C1 established from SJ-N-CG cells. All, $P< 0.05$. Upper left: Time course of growth of stably mock- (mock-C1 and C2) or PTGER2- (PTGER2-Myc-C1 and C2) transfected clones established from GOTO cells (Supplementary Figure S3a). Upper right: Comparison of the number of viable cells at day 4 among stable transfectants established from GOTO and SJ-N-CG cells. Lower: Expression level of transfected PTGER2 protein in each stable transfectant was determined by western blotting using anti-Myc-tag antibody. The quantification determined by densitometer is provided.

Figure 3 Methylation and expression status of *PTGER2* in primary NB tumors. (**a**) Upper, Representative results of bisulfite sequencing of the CpG islands of *PTGER2* in primary NB tumors and the normal adrenal gland as a control. See legend for Figure 2b for interpretation. Black (MSP) and white (USP) arrows indicate the positions of primer sequences designed to amplify methylated and unmethylated alleles, respectively, in MSP experiments. Closed arrow (Region 3-A) indicates commonly methylated region in cell lines and primary tumors of NB (Supplementary Figure S1). Lower, Results of MSP experiments for 49 primary NB tumors and two ganglioneuromas. DNAs from SH-SY5Y and GOTO cell lines were used for unmethylated and methylated controls, respectively. Arrowheads indicate methylated alleles. (**b**) *PTGER2* methylation status of primary NB tumors, compared with tumor stage (left) and *MYCN* amplification status (right). Methylation status was determined by MSP. Left: The *PTGER2* CpG island was methylated in four of 37 stage 1, 2, 3 or 4S tumors (10.8%), while 8 of 12 (66.7%) stage 4 tumors showed methylated alleles ($P=0.0004$, Fisher's exact test). Right: Methylation of the *PTGER2* CpG island in eight of the nine tumors (88.9%) with *MYCN* amplification; only four of 40 (10%) tumors without *MYCN* amplification show methylated alleles ($P<0.0001$, Fisher's exact test). (**c**) Expression of *PTGER2* mRNA in 39 primary NB tumors, compared with methylation status of the *PTGER2* Region 3 (left) and *MYCN* amplification status (right). The levels of *PTGER2* mRNA expression were determined by real-time quantitative RT–PCR experiments. Median values are indicated with horizontal bars in the boxes. The vertical bars indicate the range and the horizontal boundaries of the boxes represent the first and third quartiles. The number of cases in each group is in parentheses. Statistical analysis used the Student's *t*-test. The number of cases in each group is in parentheses. (**d–g**) Representative immunohistochemical analysis of PTGER2 protein using specific antibody. (**d**) Ganglioneuroma. Matured ganglion cells showed strong PTGER2 immunoreactivity. (**e**) Stage 1 tumors of NB with good prognosis. NB cells differentiating to ganglion-like cells showed strongly PTGER2 immunoreactivity, whereas undifferentiated small round cells showed weak PTGER2 immunoreactivity. (**f** and **g**) Stage 4 NB tumors with *MYCN* amplification. Undifferentiated small round cells showed very weak or no PTGER2 immunoreactivity. Note that nontumorous mesenchymal cells, including endothelial cells and infiltrating cells such as lymphocytes and macrophages, were strongly stained for PTGER2.

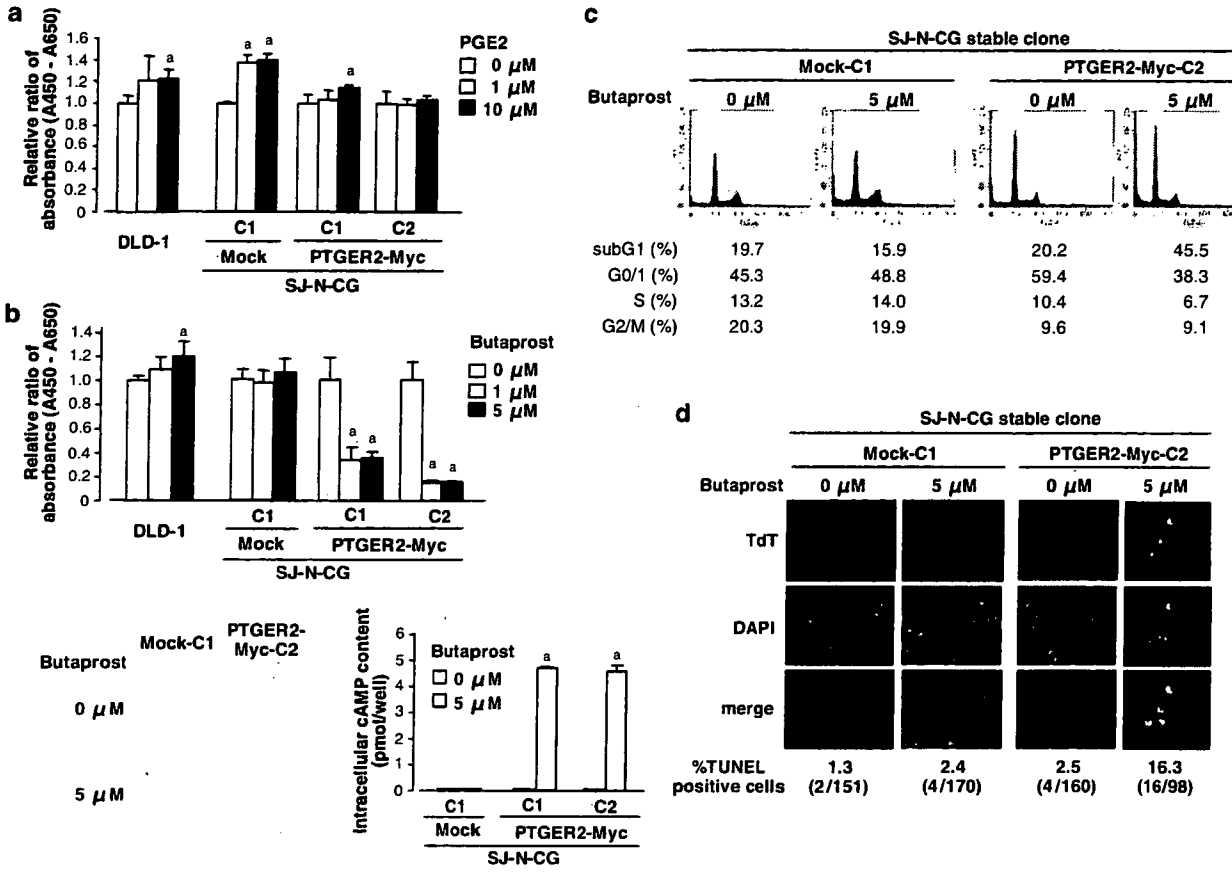

Figure 5 Inhibition of NB cell growth by PTGER2-mediated signaling. (**a**) Effect of PGE2 on growth of NB cells stably expressing PTGER2. After preculture for 24 h in medium containing 1% FBS, stable mock (mock-C1) or PTGER2 (PTGER2-Myc-C1 and C2) transfectants established from SJ-N-CG cells were treated with 0, 1, or 10 μM of PGE2 for 3 days and cell viability was determined by WST assay. The effect of PGE2 on cell growth was shown by absorbance of PGE2-treated cells relative to that of vehicle-treated cells (relative ratio). Statistical analysis used one-way ANOVA with subsequent Scheffé's tests: (**a**) $P<0.05$ versus cells treated with vehicle alone. Note that DLD-1, a colorectal-cancer cell line whose growth is promoted by PGE2 through a PTGER2-mediated signaling pathway other than a cAMP-dependent one, showed an increase in cell numbers after treatment with PGE2 for 72 h. (**b**) Effect of a specific PTGER2 agonist, butaprost, on growth and levels of intracellular cAMP in NB cells stably expressing PTGER2. Left, after preculture for 24 h in medium containing 1% FBS, stable mock (mock-C1) or PTGER2 (PTGER2-Myc-C1 and C2) transfectants established from SJ-N-CG cells were treated with 0, 1, or 5 μM of butaprost for 3 days and cell viability was determined by WST assay. The effect of butaprost on cell growth is shown as a relative ratio, as described in (**a**). Statistical analysis used one-way ANOVA with subsequent Scheffé's tests: (**a**) $P<0.05$ versus cells treated with vehicle alone. Note that DLD-1 showed an increase in cell numbers after treatment with butaprost for 72 h. Right: after 24-h preculture in medium containing 1% FBS, stable mock (mock-C1) or PTGER2 (PTGER2-Myc-C1 and C2) transfectants established from SJ-N-CG cells were treated with 0 or 5 μM of butaprost for 20 min. Levels of intracellular cAMP were determined by a cAMP EIA system (GE Healthcare Bio-Sciences, Piscataway, NJ, USA) according to the manufacturer's protocol. Statistical analysis used the Mann–Whitney *U*-test; (**a**) $P<0.05$ versus vehicle-treated control cells. (**c**) FACS analysis of PTGER2-stable transfectant (PTGER2-Myc-C2) and control clones (mock-C2). PTGER2-stable transfectants established from SJ-N-CG cells accumulated in G_0–G_1 phase in comparison with control clones. Notably, an increase in the sub-G_1 fraction and a decrease in the G_2/M fraction were observed in butaprost-treated PTGER2 transfectants. (**d**) Representative image of TUNEL staining in stable mock (mock-C1) and PTGER2 (PTGER2-Myc-C2) transfectants of SJ-N-CG with or without butaprost treatment. More TUNEL-positive cells were detected in stable PTGER2 transfectants treated with 5 μM of butaprost (16.3%) than in transfectants treated with vehicle alone (2.5%); the number of TUNEL-positive cells in mock-transfectant cultures was not affected by butaprost. Magnifications are × 400.

histone modification, especially in *MYCN*-amplified cells. Methylation of *PTGER2* was also observed in advanced primary NB tumors, although its direct correlation with expression status in primary NBs remains unclear due to high expression levels of *PTGER2* in unavoidable nontumor cells. Growth of NB cell lines lacking expression of *PTGER2* was inhibited by exogenous restoration of the gene product. Moreover, a PTGER2-specific agonist inhibited growth of transfected NB cell lines that were stably expressing exogenous PTGER2, at least in part through production of cAMP as a second messenger in those cells.

PTGER2 locates in 14q22.1, a chromosomal region that is involved in loss of heterozygosity (LOH) or copy-number losses in 20–25% of NBs, although the smallest region of overlapping LOH at 14q is more distal (14q23-qter; Thompson *et al.*, 2001). Indeed, most of the cell lines we used in this study showed normal copy numbers

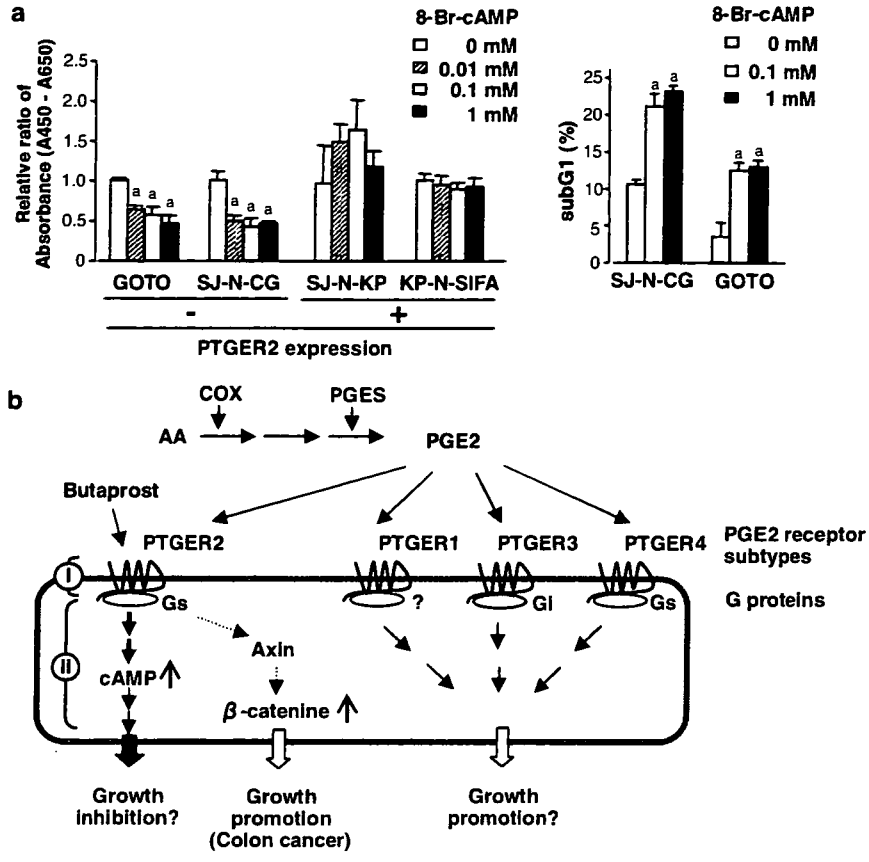

Figure 6 (a) Left: Effect of a cell-permeable cAMP analog, 8-Br-cAMP, on growth of NB cells. Wild-type GOTO and SJ-N-CG cells, which lack expression of *PTGER2*, and SJ-N-KP and KP-N-SIFA, which do express the gene, were cultured for 72 h with various concentrations of 8-Br-cAMP or no 8-Br-cAMP, and cell viability was determined by WST assay. The effect of 8-Br-cAMP on cell growth is shown as a relative ratio, as described for (a). Statistical analysis used one-way ANOVA with subsequent Scheffé's tests: (a) $P<0.05$ versus cells treated with vehicle alone. Notably, 8-Br-cAMP inhibited cell growth in GOTO and SJ-N-CG cells, but not in SJ-N-KP and KP-N-SIFA. Right: An increase in sub-G_1 fraction was observed after treatment with 8-Br-cAMP in GOTO and SJ-N-CG cells. Wild-type GOTO and SJ-N-CG cells, which lack expression of *PTGER2*, were cultured with 0, 0.1, or 1.0 mM of 8-Br-cAMP for 72 h. The data presented are the means ± s.d. of three separate experiments. Statistical analysis used one-way ANOVA with subsequent Scheffé's tests: (a) $P<0.05$ versus 0 mM of 8-Br-cAMP treated cells. (b) Schematic representation of interactions among PTGER2 signals and cell growth. COX, cyclo-oxygenase; PGES, prostaglandin E synthase. The PTGRE2 signaling pathway may be disrupted in NB cells through epigenetic silencing of *PTGRE2* (I). Alternatively or in addition, disruption of downstream signaling, including unresponsiveness to cAMP (II), may contribute to loss of the tumor-suppressive activity of normal PGE2-PTGRE2 signaling.

at 14q22 in conventional (Saito-Ohara *et al.*, 2003) and BAC array-based (unpublished data) comparative genomic hybridization (CGH) experiments, suggesting that homozygous inactivation of *PTGER2* might occur through biallelic DNA methylation/histone modification in NB cells.

The putative 'core promoter region' of *PTGER2*, which showed high promoter activity in our reporter assay, was not methylated in some of the NB cell lines we analysed regardless of the gene's expression status, although aberrant DNA methylation in exonic region (Region 3) of *PTGER2* was inversely correlated with expression in NB cell lines. On the other hand, within the putative 'core promoter region' the acetylation status of H3 and H4 histones, and the di- and trimethylation status of H3K9, were positively and inversely correlated with *PTGER2* expression, respectively. In view of these observations, we speculate that silencing of *PTGER2* in NB cells depends on integrated epigenetic events such as DNA methylation and histone modification. This phenomenon has been observed in other genes, including tumor-suppressor genes among a variety of solid tumors (Nakagawachi *et al.*, 2003; Stirzaker *et al.*, 2004; Strunnikova *et al.*, 2005; Frigola *et al.*, 2006; Yamada *et al.*, 2006).

Epigenetic mechanisms of tumor-suppressor-gene silencing in cancer remains incompletely understood (Jones and Baylin, 2002). It is believed that DNA sequences in entire CpG islands with promoter activity are methylated, H3 and H4 are unacetylated and H3K9 is methylated. However, it was also reported that hypermethylation of nonpromoter exonic sequences affects heterochromatinization and local gene silencing (Frigola *et al.*, 2006). In some cancer-associated gene silencing, moreover, sequences outside the promoter region may be methylated first (Jones and Baylin, 2002;

Nakagawachi *et al.*, 2003; Stirzaker *et al.*, 2004; Strunnikova *et al.*, 2005;), and this methylation could induce histone modifications such as deacetylation of lysine residues by histone deacetylase and H3K9 di- and tri-methylation by histone methyltransferase (Kondo *et al.*, 2003; Stirzaker *et al.*, 2004; Strunnikova *et al.*, 2005), mediated by methyl-CpG-binding proteins. These processes lead to condensation of the chromatin, which propagates into a transcription factor-binding region, making target sequences inaccessible to transcription factors; finally gene transcription is shut off (Jones and Baylin, 2002; Nakagawachi *et al.*, 2003). Consequently, methylation outside the promoter region could lead gene silencing indirectly, although histone modification within the critical promoter region may contribute to silencing directly. This scenario is consistent with our results showing that TSA alone can partially restore expression of *PTGER2* and that TSA and 5-aza-dCyd exert a synergistic effect on restoring expression of this gene.

Using primary NB tumors, we showed that *PTGER2* methylation within Region 3 occured more frequently in aggressive NBs such as stage 4 tumors than early-stage tumors, and in tumors with *MYCN* amplification than tumors without its amplification. Therefore the methylation status of this gene might be useful for predicting the aggressiveness of NB tumors, although our set of tumors was not suitable for survival analysis because few of the patients died during the follow-up period. Since PTGER2 is expressed in nontumorous cells, such as endothelial cells, and also in infiltrating lymphocytes and macrophages, it will be difficult to evaluate correlation between silenced *PTGER2* expression and methylation status of NB cells in clinical samples. To clarify the clinical significance of the *PTGER2* gene in NB, further examination of methylation status, not expression status, of this gene in a larger set of primary cases of NB will be required.

One of the most striking findings in the study reported here is that restoration of PTGER2 protein by either transient or stable transfection of expression constructs inhibited growth of NB cells that lacked endogenous *PTGER2*. Moreover, a PTGER2-specific agonist (butaprost) inhibited growth of NB cells stably expressing exogenous PTGER2, at least partly by inducing apoptosis. Those results suggested that negative regulation of cell growth, including induction of apoptosis, was a significant consequence of ectopic expression of PTGER2 in NB cells lacking expression of this gene.

PGE2 is biosynthesized from arachidonic acid as a major cyclo-oxygenase product in a number of physiological settings, and produces a broad range of biologic actions in diverse tissues (Narumiya *et al.*, 1999). It was shown that cyclo-oxygenase-2 (COX-2) is expressed in NB, and COX-inhibiting nonsteroidal anti-inflammatory drugs inhibit growth of NB cells *in vitro* and *in vivo* (Johnsen *et al.*, 2004). In some tumors, including colon cancer, PGE2 has been implicated in promotion of tumor growth, promotion of angiogenesis, inhibition of apoptosis, stimulation of invasion, or suppression of immune responses (Hoshino *et al.*, 2003; Hata and Breyer, 2004; Castellone *et al.*, 2005; Wang *et al.*, 2005a, 2006; Wang and DuBois, 2006). Those activities indicate that genes encoding receptors for PGE2 and/or its downstream targets can act as oncogenes. However, PGE2 can also act anti-proliferatively in some tumors, inducing apoptosis or differentiation (Santoro *et al.*, 1977; Fulton *et al.*, 1989; Fedyk *et al.*, 1996; Okuyama *et al.*, 2002), indicating that receptors for PGE2 and/or its downstream targets also can function as tumor suppressors.

Signaling of PGE2 is mediated by four receptors (PTGRE 1–4); the physiological/pathophysiological behavior of PGE2 appears to depend on the type of its receptors and on downstream pathways, accounting for completely opposite effects (Narumiya *et al.*, 1999). Although an antiapoptotic effect of PTGER2 in gastric mucosal cells (Hoshino *et al.*, 2003) and a growth-promoting effect in colon-cancers via the PTGER2-G_s-axin-β-catenin signaling pathway (Castellone *et al.*, 2005) have been reported, several lines of evidence show that PTGER2 also can negatively regulate cell growth and induce apoptosis and/or differentiation in various types of cells (Fedyk *et al.*, 1996; Suda *et al.*, 1996; Okuyama *et al.*, 2002). Thus, the role played by the PGE2-PTGER2 signaling pathway may vary considerably from one neoplasm to another, probably in a tissue- or cell lineage-dependent manner. This hypothesis is consistent with our results demonstrating that butaprost promoted cell growth in colon-cancer cell line DLD-1, as expected on the basis of published data (Castellone *et al.*, 2005), but inhibited growth of NB cells stably expressing PTGER2. In NB, disruption of the PTGER2-mediated growth-suppressive pathway may contribute to tumor progression.

The question of how the cellular context is able to determine the action of PGE2-PTGER2 signaling in NB cells is extremely interesting and deserves further investigation. PGE2 increases intracellular concentrations of cAMP through PTGER2 and PTGER4 and some splice variants of PTGER3, coupling to G proteins (Narumiya *et al.*, 1999). Among PGE2 receptors, PTGER2 has the most potential for elevating intracellular cAMP concentrations (Regan, 2003). Since elevated levels of cAMP are associated with decreased proliferation and increased differentiation or apoptosis in several types of cells including glioblastoma cells (Chen *et al.*, 1998), esophageal squamous cell carcinomas (Wang *et al.*, 2005b), and hippocampal cells (Takadera *et al.*, 2004), we speculate that PTGER2-mediated production of intracellular cAMP may contribute to the growth-inhibitory effect of restored PTGER2 in NB cells lacking endogenous expression of the gene. In our experiments a PTGER2-specific agonist increased intracellular cAMP levels and exerted growth inhibitory effects, at least partly by inducing apoptosis, in stable PTGER2 transfectants established from the SJ-N-CG cell line, although G_0–G_1 arrest but not apoptosis was predominantly observed in PTGER2 transfectants under low-serum condition without butaprost treatment. A similar effect of butaprost in hippocampal cells has been reported (Takadera *et al.*,

2004), even though those cells were nontumorous. The fact that a cAMP analog, 8-Br-cAMP, which directly increases intracellular cAMP, inhibited cell growth and induced apoptosis in NB cells lacking endogenous PTGER2, but not in those expressing PTGER2, suggested that NB cells may lose responsiveness to PTGER2-mediated growth inhibition/apoptosis through epigenetic silencing of PTGER2 (I in Figure 6b) or by disruption of a downstream cAMP-dependent signaling pathway (II in Figure 6b). Further examination will be needed to clarify the biological and clinical significance of the PGE2-PTGER2-cAMP signaling pathway in the pathogenesis of NB, especially with regard to the resistance of advanced NB tumors to apoptosis (del Carmen Mejia *et al.*, 2002).

Materials and methods

Cell culture and primary tissue samples

All 20 human NB cell lines we used (SJ-N-KP, SK-N-AS, SK-N-SH, SH-SY5Y, KP-N-SILA, KP-N-SIFA, MP-N-TS, MP-N-MS, SMS-KCN, SMS-KAN, NB-1, CHP134, SJ-N-CG, SK-N-DZ, IMR32, GOTO, KP-N-YN, KP-N-RT, KP-N-TK, KP-N-YS) had been established from surgically resected tumors (Saito-Ohara *et al.*, 2003). The DLD-1 colon-cancer cell line was purchased from the Japanese Collection of Research Bioresources (Osaka, Japan). Cells were maintained in RPMI-1640, supplemented with 10% fetal bovine serum (FBS) and 100 U/ml penicillin/100 μg/ml streptomycin. NB cells were treated with or without 1 or 5 μM of 5-aza-dCyd for 5 days, and/or 100 ng/ml of TSA for the last 12 h.

Primary tumor samples were obtained at surgery from 49 patients with NB and two with ganglioneuroma who underwent tumor resection at University Hospital, Kyoto Prefectural University of Medicine from 1986 to 2003, with written consent from the parents of each patient in the formal style and after approval by the local ethics committees. Staging of each NB case was determined according to the criteria of the International Neuroblastoma Staging System (Brodeur *et al.*, 1993). Of the 49 NB patients, 41 (83.7%) were infants less than 18 months of age at diagnosis, 36 (73.5%) were detected by a mass-screening program, 12 were classified as stage 1, 11 as stage 2, nine as stage 3, 12 as stage 4 and five as stage 4S; *MYCN* amplification was detected in the tumors of nine (18.4%) patients. Genomic DNA was available for analysis from all 49 NB and two ganglioneuroma samples; total RNA was available from 39 NB samples.

Reagents and plasmids

PGE2, butaprost and 8-Br-cAMP were obtained respectively from Calbiochem (San Diego, CA, USA), Cayman Chemicals (Ann Arbor, MI, USA) and Sigma-Aldrich (St Louis, MO, USA). Anti-PTGER2 polyclonal antibody was from Cayman Chemicals. Anti-acetylated histone H3 (anti-AcH3), anti-acetylated histone H4 (anti-AcH4), anti-dimethylated histone H3 lysine 9 (anti-2Me-H3K9) and anti-trimethylated histone H3 lysine 9 (anti-3Me-H3K9) antibodies were from Upstate (Lake Placid, NY, USA); anti-Myc-tag and anti-p44/42 antibodies were from Cell Signaling Technology (Beverly, MA, USA).

Plasmids expressing PTGER2 alone (pcDNA3.1-*PTGER2*) C-terminally Myc-tagged PTGER2 (pcDNA3.1-*PTGER2*-Myc) were prepared by cloning the RT–PCR product of the full coding sequence of *PTGER2* alone, or in-frame along with the Myc-epitope in the C terminus, respectively, into the vector pcDNA3.1 (Invitrogen, Carlsbad, CA, USA). The empty vector pcDNA3.1 or plasmid expressing Myc-tagged GFP (pcDNA3.1-GFP-Myc) was used as a control.

RT–PCR and real-time quantitative RT–PCR

Single-stranded cDNAs generated from total RNAs were amplified with primers specific for each gene (Supplementary Table S1). The glyceraldehyde-3-phosphate dehydrogenase gene (*GAPDH*) was amplified at the same time to allow estimation of the efficiency of cDNA synthesis. RT–PCR products were electrophoresed, and quantified with LAS-3000 (Fujifilm, Tokyo, Japan). Levels of mRNA expression in primary tumors were measured using a quantitative real-time fluorescence detection method (PRISM 7900HT, Applied Biosystems, Foster City, CA, USA) according to the manufacturer's protocol. The expression of *PTGER2* mRNA in each sample was normalized on the basis of the respective *GAPDH* content and recorded as a relative expression level. PCR amplification was performed in duplicate for each sample.

Methylation analysis

Genomic DNAs were treated with sodium bisulfite, and subjected to PCR using primer sets designed to amplify regions of interest (Supplementary Table S1). For COBRA, PCR products were digested with *Taq*I, and electrophoresed (Xiong and Laird, 1997). For bisulfite sequencing, the PCR products were subcloned and then sequenced.

For MSP, sodium bisulfite-treated DNA was amplified using primers specific to the methylated and unmethylated forms of DNA sequences (Supplementary Table S1). DNAs from cell lines recognized as unmethylated or highly methylated by bisulfite sequencing were used as controls.

Promoter assay

DNA fragments around the CpG-island predicted by the CpGPLOT program (http://www.ebi.ac.uk/emboss/cpgplot/) were ligated into the vector pGL3-Basic (Promega, Madison, WI, USA). Promoter assay using each construct or control vector with an internal control vector (pRL-hTK, Promega) was performed as described elsewhere (Misawa *et al.*, 2005).

ChIP assay

ChIP assays were performed as described previously (Sonoda *et al.*, 2004). Chromatin was immunoprecipitated with anti-AcH3, anti-AcH4, anti-2Me-H3K9, anti-3Me-H3K9, or no antibody, after which a quantitative real-time PCR was performed with 1/30 of the immunoprecipitated DNA, using primers designed to amplify regions of interest (Supplementary Table S1); 1/600 of the solution before adding antibody was amplified as an internal control for the amount of DNA.

Immunohistochemistry

Formalin-fixed, paraffin-embedded surgical specimens were sliced into 5 μm-thick sections, deparaffinized, then immersed for 30 min in methanol containing 0.3%. hydrogen peroxide. After retrieval of epitope by boiling, the sections were incubated with anti-PTGER2 antibody (1:500 dilution) and then with a biotinylated secondary antibody (1:200 dilution; Vector Laboratories, Burlingame, CA, USA). After staining with Vectastain ABC reagent (Vector Laboratories), the sections were immersed in 0.05% diaminobenzidine tetrahydrochloride solution containing 0.01% hydrogen peroxide, and counterstained with hematoxylin.

Transient transfection and colony-formation assays
pcDNA3.1-*PTGER2*, pcDNA3.1-*PTGER2*-Myc or the empty-vector (pcDNA3.1-mock) were transiently transfected into SJ-N-CG and GOTO cells using FuGENE6 (Roche Diagnostics, Tokyo, Japan) for colony-formation assays. Expression of PTGER2 protein in transfected cells was confirmed by western blotting, using anti-Myc-Tag or anti-PTGER2 antibody as described elsewhere (Misawa *et al.*, 2005). After 2–3 weeks of incubation with G418 (600 and 250 μg/ml for SJ-N-CG and GOTO, respectively), cells were stained with crystal violet.

Immunofluorescent staining
Transiently or stably transfected cells seeded into slide chambers were fixed in cold methanol for 3 min. The cells were covered with blocking solution (1% skim milk in phosphate-buffered saline) for 30 min, and incubated overnight at 4°C with anti-Myc-tag antibody (1:200 dilution) in blocking solution. There followed 1 h of incubation with Alexa 594-conjugated goat anti-mouse IgG (1:500 dilution; Molecular Probes, Eugene, OR, USA). The cells were counterstained with 4′,6-diamidino-2-phenylindole, and viewed with an ECLIPSE E800 fluorescence microscope (Nikon, Tokyo, Japan).

Establishment of stable transfectants and cell-growth assay
Stable transfectants of *PTGER2* and mock vector were obtained by transfecting pcDNA3.1-*PTGER2*-Myc. and pcDNA3.1-mock, respectively, into SJ-N-CG and GOTO cells, and selected by G418. For measurements of cell growth, 2×10^3 cells were seeded in 96-well plates. To determine the effects of PGE2, butaprost, or 8-Br-cAMP on growth of NB cells, wild type cell lines or stable transfectants of SJ-N-CG cells were treated with various concentrations of each reagent for 72 h, after 24-h preculture in media containing 1% FBS (for PGE2 and butaprost) or 10% FBS (for 8-Br-cAMP). The numbers of viable cells were assessed by a colorimetric water-soluble tetrazolium salt (WST) assay as described elsewhere (Misawa *et al.*, 2005). The DLD-1 cell line was served as a positive control for the PGE2 and butaprost experiments (Castellone *et al.*, 2005).

Enzyme immunoassay
After 24-h pre-culture in medium containing 1% FBS, stable transfectants of SJ-N-CG cells were treated with 0 or 5 μM of butaprost for 20 min. Intracellular cAMP was measured by means of a cAMP Enzyme immunoassay (EIA) system (GE Healthcare Bio-Sciences, Piscataway, NJ, USA) according to the manufacturer's protocol.

Flow cytometry
Stable transfectants of SJ-N-CG cells were treated with butaprost (5 μM) or 8-Br-cAMP (0.1 or 1 mM) for 72 h. For FACS analysis, harvested cells were fixed in 70% cold ethanol before treatment with RNaseA and propidium iodide. Samples were analysed on a FACSCalibur HG (Becton-Dickinson, San Jose, CA, USA). Data were analysed using BD CellQuest Pro (Becton-Dickinson).

TUNEL stain
Wild-type or stable transfectants of SJ-N-CG cells were treated with or without butaprost or 8-Br-cAMP, and apoptosis was detected by enzymatic labeling of DNA strand-breaks using a TUNEL staining kit (MEBSTAIN Apoptosis Kit Direct; MBL, Aichi, Japan) according to the manufacturer's protocol.

Acknowledgements

This work was supported by Grants-in-Aid for Scientific Research on Priority Areas (C) from the Ministry of Education, Culture, Sports, Science and Technology, Japan; by a Grant-in-Aid from Core Research for Evolutional Science and Technology (CREST) of the Japan Science and Technology Corporation (JST); and by a 21st Century Center of Excellence (COE) Program for Molecular Destruction and Reconstitution of Tooth and Bone.

References

Abe M, Ohira M, Kaneda A, Yagi Y, Yamamoto S, Kitano Y *et al.* (2005). CpG island methylator phenotype is a strong determinant of poor prognosis in neuroblastomas. *Cancer Res* **65**: 828–834.

Azuara V, Perry P, Sauer S, Spivakov M, Jorgensen HF, John RM *et al.* (2006). Chromatin signatures of pluripotent cell lines. *Nat Cell Biol* **8**: 532–538.

Brodeur GM, Pritchard J, Berthold F, Carlsen NL, Castel V, Castelberry RP *et al.* (1993). Revision of the international criteria for neuroblastoma diagnosis, staging, and response to treatment. *J Clin Oncol* **11**: 1466–1477.

Brodeur GM. (2003). Neuroblastoma: biological insights into a clinical enigma. *Nat Rev Cancer* **3**: 203–216.

Castellone MD, Teramoto H, Williams BO, Druey KM, Gutkind JS. (2005). Prostaglandin E2 promotes colon cancer cell growth through a GS-axin-beta-catenin signaling axis. *Science* **310**: 1504–1510.

Chen TC, Hinton DR, Zidovetzki R, Hofman FM. (1998). Up-regulation of the cAMP/PKA pathway inhibits proliferation, induces differentiation, and leads to apoptosis in malignant gliomas. *Lab Invest* **78**: 165–174.

del Carmen Mejia M, Navarro S, Pellin A, Ruiz A, Castel V, Llombart-Bosch A. (2002). Study of proliferation and apoptosis in neuroblastoma. Their relation with other prognostic factors. *Arch Med Res* **33**: 466–472.

Fedyk ER, Ripper JM, Brown DM, Phipps RP. (1996). A molecular analysis of PGE receptor (EP) expression on normal and transformed B lymphocytes: coexpression of EP1, EP2, EP3beta and EP4. *Mol Immunol* **33**: 33–45.

Frigola J, Song J, Stirzaker C, Hinshelwood RA, Peinado MA, Clark SJ. (2006). Epigenetic remodeling in colorectal cancer results in coordinate gene suppression across an entire chromosome band. *Nat Genet* **38**: 540–549.

Fulton AM, Laterra JJ, Hanchin CM. (1989). Prostaglandin E2 receptor heterogeneity and dysfunction in mammary tumor cells. *J Cell Physiol* **139**: 93–99.

Hata AN, Breyer RM. (2004). Pharmacology and signaling of prostaglandin receptors: Multiple roles in inflammation and immune modulation. *Pharmacol Ther* **103**: 147–166.

Hoshino T, Tsutsumi S, Tomisato W, Hwang HJ, Tsuchiya T, Mizushima T. (2003). Prostaglandin E2 protects gastric mucosal cells from apoptosis via EP2 and EP4 receptor activation. *J Biol Chem* **278**: 12752–12758.

Inazawa J, Inoue J, Imoto I. (2004). Comparative genomic hybridization (CGH)-arrays pave the way for identification of novel cancer-related genes. *Cancer Sci* **95**: 559–563.

Johnsen JI, Lindskog M, Ponthan F, Pettersen I, Elfman L, Orrego A *et al.* (2004). Cyclooxygenase-2 is expressed in neuroblastoma, and nonsteroidal anti-inflammatory drugs

induce apoptosis and inhibit tumor growth *in vivo*. *Cancer Res* **64**: 7210–7215.
Jones PA, Baylin SB. (2002). The fundamental role of epigenetic events in cancer. *Nat Rev Genet* **3**: 415–428.
Kondo Y, Shen L, Issa JP. (2003). Critical role of histone methylation in tumor suppressor gene silencing in colorectal cancer. *Mol Cell Biol* **23**: 206–215.
Lorincz MC, Dickerson DR, Schmitt M, Groudine M. (2004). Intragenic DNA methylation alters chromatin structure and elongation efficiency in mammalian cells. *Nat Struct Mol Biol* **11**: 1068–1075.
Misawa A, Inoue J, Sugino Y, Hosoi H, Sugimoto T, Hosoda F *et al.* (2005). Methylation-associated silencing of the Nuclear Receptor 1I2 gene in advanced-type Neuroblastomas, Identified by Bacterial Artificial Chromosome Array-Based Methylated CpG Island Amplification. *Cancer Res* **65**: 10233–10242.
Nakagawachi T, Soejima H, Urano T, Zhao W, Higashimoto K, Satoh Y *et al.* (2003). Silencing effect of CpG island hypermethylation and histone modifications on O6-methylguanine-DNA methyltransferase (MGMT) gene expression in human cancer. *Oncogene* **22**: 8835–8844.
Narumiya S, Sugimoto Y, Ushikubi F. (1999). Prostanoid receptors: structures, properties, and functions. *Physiol Rev* **79**: 1193–1226.
Okuyama T, Ishihara S, Sato H, Rumi MA, Kawashima K, Miyaoka Y *et al.* (2002). Activation of prostaglandin E2-receptor EP2 and EP4 pathways induces growth inhibition in human gastric carcinoma cell lines. *J Lab Clin Med* **140**: 92–102.
Regan JW. (2003). EP2 and EP4 prostanoid receptor signaling. *Life Sci* **74**: 143–153.
Saito-Ohara F, Imoto I, Inoue J, Hosoi H, Nakagawara A, Sugimoto S *et al.* (2003). PPM1D Is a Potential Target for 17q Gain in Neuroblastoma. *Cancer Res* **63**: 1876–1883.
Santoro MG, Philpott GW, Jaffe BM. (1977). Inhibition of B-16 melanoma growth *in vivo* by a synthetic analog of prostaglandin E2. *Cancer Res* **37**: 3774–3779.
Schubeler D, Lorincz MC, Cimbora DM, Telling A, Feng YQ, Bouhassira EE *et al.* (2000). Genomic targeting of methylated DNA: influence of methylation on transcription, replication, chromatin structure, and histone acetylation. *Mol Cell Biol* **20**: 9103–9112.
Sonoda I, Imoto I, Inoue J, Shibata T, Shimada Y, Chin K *et al.* (2004). Frequent silencing of low density lipoprotein receptor-related protein 1B (LRP1B) expression by genetic and epigenetic mechanisms in esophageal squamous cell carcinoma. *Cancer Res* **64**: 3741–3747.
Stirzaker C, Song JZ, Davidson B, Clark SJ. (2004). Transcriptional gene silencing promotes DNA hypermethylation through a sequential change in chromatin modifications in cancer cells. *Cancer Res* **64**: 3871–3877.
Strunnikova M, Schagdarsurengin U, Kehlen A, Garbe JC, Stampfer MR, Dammann R. (2005). Chromatin inactivation precedes *de novo* DNA methylation during the progressive epigenetic silencing of the RASSF1A promoter. *Mol Cell Biol* **25**: 3923–3933.
Suda M, Tanaka K, Natsui T, Usui T, Tanaka I, Fukushima M *et al.* (1996). Prostaglandin E receptor subtypes in mouse osteoblastic cell line. *Endocrinology* **137**: 1698–1705.
Takadera T, Shiraishi Y, Ohyashiki T. (2004). Prostaglandin E2 induced caspase-dependent apoptosis possibly through activation of EP2 receptors in cultured hippocampal neurons. *Neurochem Int* **45**: 713–719.
Teitz T, Wei T, Valentine MB, Vanin EF, Grenet J, Valentine VA *et al.* (2000). Caspase 8 is deleted or silenced preferentially in childhood neuroblastomas with amplification of MYCN. *Nat Med* **6**: 529–535.
Thompson PM, Seigfried BA, Kyemba SK, Jensen SJ, Guo C, Maris JM *et al.* (2001). Loss of heterozygosity for chromosome 14q in neuroblastoma. *Med Pediatr Oncol* **36**: 28–31.
Toyota M, Ho C, Ahuja N, Jair KW, Li Q, Ohe-Toyota M *et al.* (1999). Identification of differentially methylated sequences in colorectal cancer by methylated CpG island amplification. *Cancer Res* **59**: 2307–2312.
Wang D, Buchanan FG, Wang H, Dey SK, DuBois RN. (2005a). Prostaglandin E2 enhances intestinal adenoma growth via activation of the Ras-mitogen-activated protein kinase cascade. *Cancer Res* **65**: 1822–1829.
Wang D, DuBois RN. (2006). Prostaglandins and cancer. *Gut* **55**: 115–122.
Wang D, Wang H, Brown J, Daikoku T, Ning W, Shi Q *et al* (2006). CXCL1 induced by prostaglandin E2 promotes angiogenesis in colorectal cancer. *J Exp Med* **203**: 941–951.
Wang HM, Zheng NG, Wu JL, Gong CC, Wang YL. (2005b). Dual effects of 8-Br-cAMP on differentiation and apoptosis of human esophageal cancer cell line Eca-109. *World J Gastroenterol* **11**: 6538–6542.
Westermann F, Schwab M. (2002). Genetic parameters of neuroblastomas. *Cancer Lett* **184**: 127–147.
Wolffe AP, Matzke MA. (1999). Epigenetics: regulation through repression. *Science* **286**: 481–486.
Xiong Z, Laird PW. (1997). COBRA: a sensitive and quantitative DNA methylation assay. *Nucleic Acids Res* **25**: 2532–2534.
Yamada N, Hamada T, Goto M, Tsutsumida H, Higashi M, Nomoto M *et al.* (2006). MUC2 expression is regulated by histone H3 modification and DNA methylation in pancreatic cancer. *Int J Cancer* **119**: 1850–1857.
Yan P, Muhlethaler A, Bourloud KB, Beck MN, Gross N. (2003). Hypermethylation-mediated regulation of CD44 gene expression in human neuroblastoma. *Gene Chromosome Cancer* **36**: 129–138.
Yang Q, Zage P, Kagan D, Tian Y, Seshadri R, Salwen HR *et al.* (2004). Association of epigenetic inactivation of RASSF1A with poor outcome in human neuroblastoma. *Clin Cancer Res* **10**: 8493–8500.
Yang QW, Liu S, Tian Y, Salwen HR, Chlenski A, Weinstein J *et al.* (2003). Methylation-associated silencing of the thrombospondin-1 gene in human neuroblastoma. *Cancer Res* **63**: 6299–6310.

Supplementary Information accompanies the paper on the Oncogene website (http://www.nature.com/onc).

Leukemia (2007), 1–4

www.nature.com/leu

LETTER TO THE EDITOR

DNA damage check points prevent leukemic transformation in myelodysplastic syndrome

Leukemia advance online publication, 10 May 2007;
doi:10.1038/sj.leu.2404748

Cells constantly suffer DNA damage caused by agents such as free oxygen radicals, natural ionizing radiation or unscheduled replicative stimuli induced by aberrant oncogene activation. The cellular response to these stresses plays a critical role for maintenance of genome integrity. Cellular DNA in mammalian cells under constant DNA-damaging stress always carries the risk of mutation. Initially, genetic alternations may take place in genes with potential oncogenic activity, which may then begin progression towards transformation. Oncogenic stimuli enforce cell proliferation, which requires DNA replication. Unscheduled DNA replication enforced by oncogenic stimuli activates a signal for stalled replication, leading to single-strand breaks and subsequently to double-strand breaks on DNA. This DNA damage facilitates activation of DNA damage check point pathways including ataxia telangiectasia mutated (ATM) and/or ataxia telangiectasia Rad3 related (ATR), which can then lead to cell cycle arrest, apoptosis, repair or cell senescence. However, once DNA damage has occurred in genes playing a crucial role in the DNA damage response itself, the DNA damage check point pathway is compromised and the cells acquire a growth advantage and can undergo transformation more readily. Such cells, manifesting genomic instability, thus start to proliferate and accumulate additional complex mutations. Tumorigenesis evolves stepwise in this fashion.[1,2] ATM protein kinase is activated by intermolecular autophosphorylation in response to DNA damage and initiates cellular responses thereto. This activation status of DNA damage check point can be determined by measuring phosphorylation status of histone H2AX at Ser 139 (γ-H2AX), phospho-Ser 1981 ATM and downstream Chk2 at Thr 67 and p53 at Ser 15. The phosphorylation of these substrates can be monitored by respective phospho-specific antibodies.

Myelodysplastic syndrome (MDS) is a clonal malignant hematological disorder characterized by ineffective hematopoiesis and reflects a preleukemic condition. Approximately 40–50% of MDS patients develop overt leukemia (OL) after several years of latency.[3]

An immunohistochemical study was performed to elucidate the activation status of these molecules that participate in the DNA damage response in MDS and OL. To validate our staining procedure, paraffin-embedded unirradiated and irradiated Epstein–Barr virus-transformed lymphoblastoid cell lines (EBV-LCLs) were stained using phospho-ATM, phospho-Chk2, phospho-p53 and γ-H2AX antibodies, respectively. EBV-LCL stained for phospho-ATM, phospho-Chk2, phospho-p53 and γ-H2AX only after irradiation (Supplementary Information 1). Thereafter, we applied these staining conditions to bone marrow specimens from MDS patients at different stages, including RA (10 cases), RAEB-I (13 cases), RAEB-II (8 cases) and OL (10 cases), as well as two controls. In contrast to the lack of staining of control bone marrow specimens, MDS-derived specimens did stain for phospho-ATM, phospho-Chk2, phospho-p53 and γ-H2AX (Figure 1a), respectively. Phospho-ATM-positive cells were also positive for phospho-Chk2 and γ-H2AX staining (Supplementary Information 2). For the phospho-ATM staining, RA samples were classified as either negative (40%) or intermediate (60%), while RAEB-I samples were classified as negative (15%), intermediate (38%) or high (47%). RAEB-II had a similar distribution, being negative (25%), intermediate (37%) or high (38%). Strong staining was also seen for phospho-Chk2 and γ-H2AX in RAEB-I and RAEB-II. Interestingly, a much lower fraction of OL showed strong staining (20%), with up to 80% of cases being negative or intermediate for phospho-ATM, phospho-Chk2 and γ-H2AX (Figure 1b). ATM phosphorylation status in nuclear extracts of MDS (RAEB-II)-derived bone marrow was also evaluated using western blotting (Figure 1c). This confirmed phosphorylation of ATM in MDS but not control bone marrow cells, supporting the findings in the immunohistochemical analyses.

A simple explanation for the discrepancy between early-(RA) and late-stage (RAEB) MDS might be that ATM signaling is not detectably activated in the early stage. Ineffective hematopoiesis in RA, however, favors a different explanation: although the ATM pathway has been activated, the activated cells have been eradicated owing to an efficient cell death signaling pathway. If this is true, RAEB-I and -II cells must have acquired aberrant survival signals such as survivin or IAP family proteins[4] associated with progression through the MDS phases, allowing ATM-activated cells to survive. Reduced activation of DNA damage check point in OL phase may support a hypothesis that leukemia progenitor cell that already had been inactivated for DNA damage check point during RAEB phase has clonally expanded.

To demonstrate that unscheduled replication causes double-strand breaks and simultaneously activates ATM in the same cells, Ki-67-stained specimens were restained with phospho-ATM antibody after stripping off the anti-Ki-67. It was observed that all Ki-67-positive cells expressed phosphorylated ATM, while some of the phospho-ATM-positive cells failed to express Ki-67 (Figure 2) suggesting prolonged ATM phosphorylation in post-mitotic G1 cells or ATM phosphorylation by cell cycle-independent genotoxic stresses.

To establish whether disease progression correlates with DNA damage check point inactivation, we studied a patient with RAEB-I who progressed to OL. Immunohistochemical studies revealed that DNA damage check point pathways were highly activated at the RAEB-I stage. Fifty percent of 100 cells randomly picked up in MDS phase were strongly stained for phospho-ATM and 20% of cells showed moderate intensity. Interestingly, none of cells in OL phase showed strong staining for phospho-ATM, but 70% of cells showed weak staining. The phosphorylation state of Chk2, p53 and H2AX was also significantly reduced on progression to OL (Figure 3a). Reduction of the phosphorylation of ATM and its downstream targets was associated with decreased staining by the generic ATM antibody in the OL sample. This suggests that ATM function was impaired in OL either by mutation of the *ATM* gene or LOH of *ATM*.

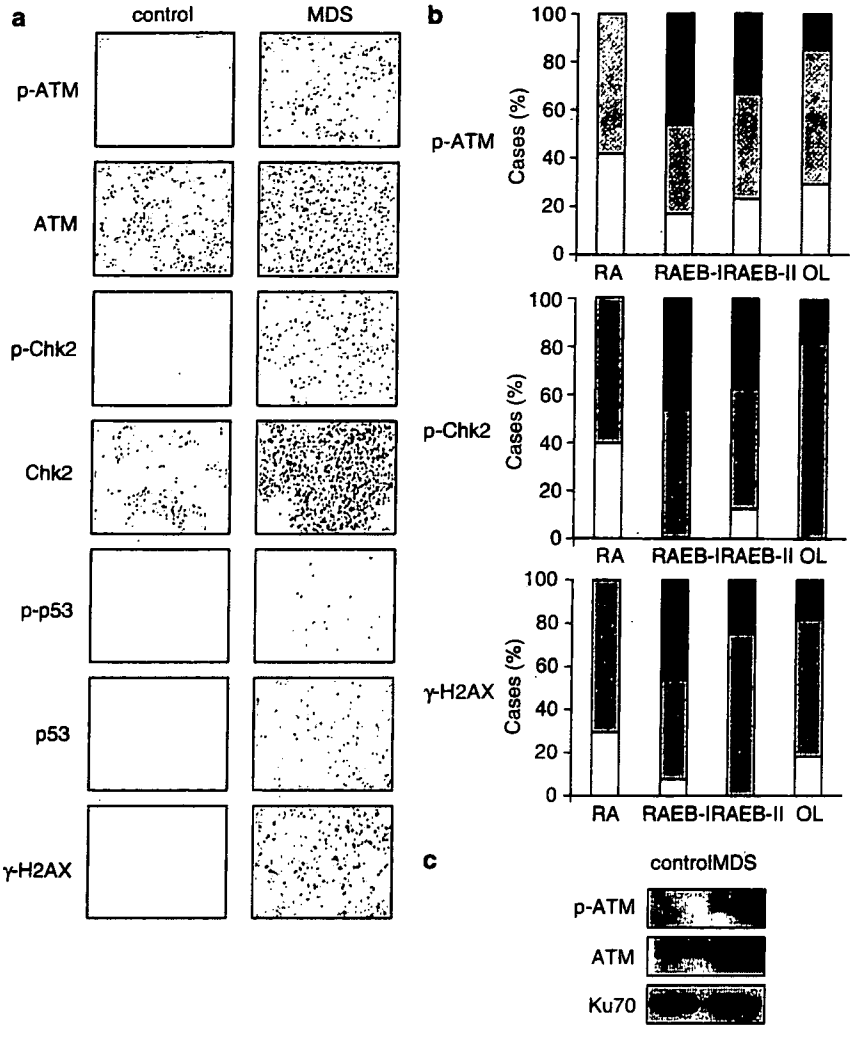

Figure 1 Activation of the ATM–Chk2–p53 pathway in bone marrow from MDS patients. (**a**) Immunohistochemical staining of control or a representative MDS (RAEB-I) bone marrow. Ser 1981-phosphorylated ATM (p-ATM), Thr 68-phosphorylated Chk2 (p-Chk2), Ser 15-phosphorylated p53 (p-p53), Ser 139 phosphorylated histone H2AX (γ-H2AX) are detectable in the MDS bone marrow sample but not in the control, despite ubiquitous expression of ATM and Chk2. (**b**) Summary of the p-ATM, p-Chk2 and γ-H2AX data in RA, RAEB-I, RAEB-II and OL. Each phosphorylated protein level is shown as either white (no expression), gray (intermediate expression) or black (high expression) bars (see Materials and methods of Supplementary Information for assignment criteria). (**c**) Western blotting of control or MDS (RAEB-II)-derived mononuclear cells. Ku70 was blotted as a nuclear extract loading control.

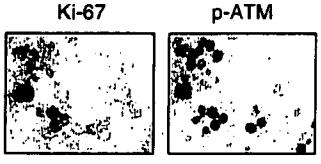

Figure 2 Dual staining of Ki-67 and phospho-ATM in MDS samples. All the Ki-67-positive cells are concomitantly stained for phosphorylated ATM, while not all the phospho-ATM-positive cells are Ki-67-positive. One of the microscopical fields showing the typical immunochemical characteristics is demonstrated. Altogether 11 cases of RA, RAEB and OL were analyzed, resulting in a similar staining pattern of Ki-67 and phospho-ATM.

Sequencing the entire *ATM* gene was impossible because only a limited amount of DNA was available from the paraffin-embedded samples. Therefore, LOH analysis of the *ATM* gene was performed by two alternative methods, one using fluorescent *in situ* hybridization (FISH) and the other by microsatellite analysis after PCR amplification. FISH analysis showed that 70% of cells at the OL stage but none in the MDS stage had lost one of the two alleles of the *ATM* gene. Microsatellite analysis using OL samples supported these FISH results (Figure 3b). Thus, ATM function was attenuated by genetic changes at the *ATM* locus during progression to OL. Both MDS and OL specimens showed strong staining with the generic p53 antibody. Accumulation of p53 in the absence of staining for phospho-p53 in OL suggests the involvement of p53 gene mutation in leukemogenesis. DNA was extracted from these specimens and each of the p53 exons was PCR-amplified and sequenced. It was found that OL bone marrow sample carried heterozygous deletions of three nucleotides at codon 572 (572del CTC, P191NA) resulting in an in-frame deletion at exon 6 (Figure 3c). In contrast, no p53 mutation was found in MDS (Figure 3c). The results from mutant-specific PCR analyses also supported these findings (data not shown).

On the basis of these observations, we draw a tentative conclusion that activation of DNA damage check point path-

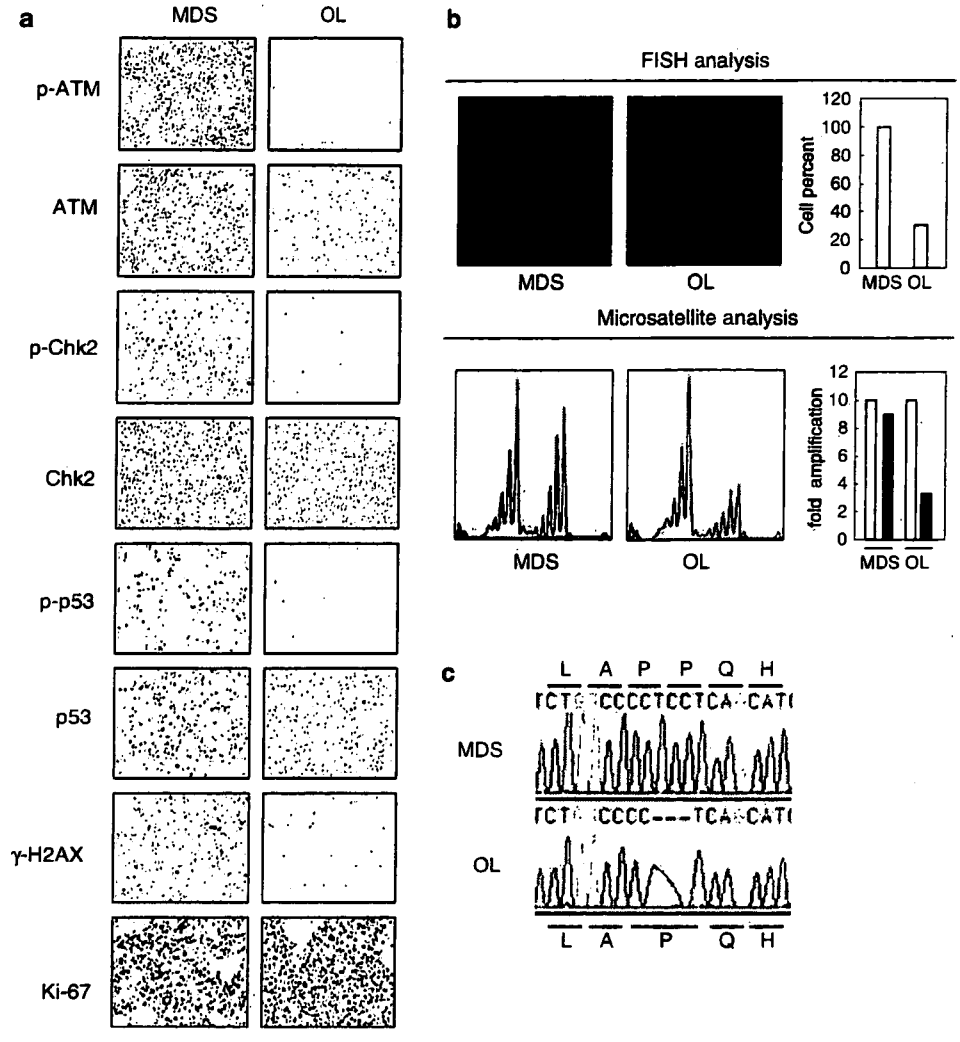

Figure 3 Immunohistochemical analyses of activation of DNA damage check points in a patient with MDS (RAEB-I) who progressed to OL. (**a**) p-ATM, p-Chk2, p-p53, γ-H2AX are strongly stained in the MDS (RAEB-I) bone marrow sample, whereas reactivity is lower in OL, despite ubiquitous expression of unphosphorylated ATM, Chk2, and p53. (**b**) Upper column: FISH analysis using *ATM* locus probe (pink) and chromosome 11 centromere probe (green) in the paired samples at MDS (RAEB-I)- or OL-phase. Percents of cells that carry biallelic ATM signals are shown as a bar graph in each phase. Lower column: Microsatellite analysis at intragenic *ATM* locus (D11S1778). Fold intensity of PCR-amplified signals was illustrated as a bar graph. The amplification signal of the deleted allele (black) was shown against that of non-deleted allele (white) standardizing the latter as 10. (**c**) Sequencing of PCR-amplified p53 exon 6 indicating a three-nucleotide in-frame deletion only in the OL sample. Sequence analysis was performed after TA cloning of PCR-amplified products. In the MDS (RAEB-I) sample, 10 of 10 amplified products showed the wild-type sequence, whereas 4 of 10 PCR products from OL showed a three-nucleotide deletion.

ways induces cell cycle arrest and/or apoptosis in MDS cells, consistent with clinically observed ineffective hematopoiesis, and that this functions as a barrier to prevent leukemic transformation. The frequency of p53 mutations in MDS is reportedly 10–15%.[5] Kitagawa *et al.*[6] suggested that p53 mutations occurring in MDS myeloid cells may confer them a growth advantage, resulting in progression to OL.

Disruption of DNA damage check points, including ATM/p53 by LOH or mutations, then results directly in evolution to OL. According to the recent concept of leukemogenic genetic events, class I and II mutations are cooperatively involved.[7] Class I comprises activating point mutations or internal tandem duplications of genes involved in signal transduction, such as tyrosine kinase receptors. Class II comprises the chromosome aberrations resulting in chimeric rearrangement of genes for hematopoietic transcription factors which disturb cellular differentiation. Although it is tempting to apply this concept to the pathogenesis of MDS, an alternative or additive genetic pathway will be required to account for the characteristic hematological features of dysplasia. In view of this two-hit model for leukemogenesis, we propose that the disruption of this DNA check point corresponds to class III mutation. This implies that 'class III' mutations allow the development of uncontrolled expansion of clinically aggressive clones in MDS. This class III mutation may even precede the chromosome translocations.[8] Our hypothesis based on these observations provides new insight into the role of DNA damage check point-related molecules in leukemogenesis.

Acknowledgements

We thank Ms Inoue and Ms Hasegawa for technical assistance. This work was supported by a Grant-in-aid from the Ministry of Education, Science and Culture. MT is supported by a Grant-in-aid from Japanese Leukemia Research Fund.

S Horibe[1], M Takagi[1,2], J Unno[1], M Nagasawa[1], T Morio[1], A Arai[3], O Miura[3], M Ohta[4], M Kitagawa[5] and S Mizutani[1]

[1]*Department of Pediatrics and Developmental Biology, Graduate School of Medicine, Tokyo Medical and Dental University, Bunkyo-ku, Tokyo, Japan;*

[2]*Department of Pediatrics, International University of Health and Welfare Mita Hospital, Minato-ku, Tokyo, Japan;*

[3]*Department of Hematology, Graduate School of Medicine, Tokyo Medical and Dental University, Bunkyo-ku, Tokyo, Japan;*

[4]*Department of Hematology, Tokyo Metropolitan Geriatric Medical Center, Itabashi-ku, Tokyo, Japan;*

[5]*Department of Comprehensive Pathology, Aging and Developmental Sciences, Graduate School of Medicine, Tokyo Medical and Dental University, Bunkyo-ku, Tokyo, Japan*

E-mail: m.takagi.ped@tmd.ac jp or smizutani.ped@tmd.ac.jp

References

1 Bartkova J, Horejsi Z, Koed K, Kramer A, Tort F, Zieger K *et al.* DNA damage response as a candidate anti-cancer barrier in early human tumorigenesis. *Nature* 2005; **434**: 864–870.

2 Gorgoulis VG, Vassiliou LV, Karakaidos P, Zacharatos P, Kotsinas A, Liloglou T *et al.* Activation of the DNA damage checkpoint and genomic instability in human precancerous lesions. *Nature* 2005; **434**: 907–913.

3 List AF, Vardiman J, Issa JP, DeWitte TM. Myelodysplastic syndromes. *Hematol Am Soc Hematol Educ Program* 2004, 297–317.

4 Yamamoto K, Abe S, Nakagawa Y, Suzuki K, Hasegawa M, Inoue M *et al.* Expression of IAP family proteins in myelodysplastic syndromes transforming to overt leukemia. *Leuk Res* 2004; **28**: 1203–1211.

5 Sugimoto K, Hirano N, Toyoshima H, Chiba S, Mano H, Takaku F *et al.* Mutations of the p53 gene in myelodysplastic syndrome (MDS) and MDS-derived leukemia. *Blood* 1993; **81**: 3022–3026.

6 Kitagawa M, Yoshida S, Kuwata T, Tanizawa T, Kamiyama R. p53 expression in myeloid cells of myelodysplastic syndromes. Association with evolution of overt leukemia. *Am J Pathol* 1994; **145**: 338–344.

7 Dash A, Gilliland DG. Molecular genetics of acute myeloid leukaemia. *Best Pract Res Clin Haematol* 2001; **14**: 49–64.

8 Nakada S, Katsuki Y, Imoto I, Yokoyama T, Nagasawa M, Inazawa J *et al.* Early G2/M checkpoint failure as a molecular mechanism underlying etoposide-induced chromosomal aberrations. *J Clin Invest* 2006; **116**: 80–89.

Supplementary Information accompanies the paper on the Leukemia website (http://www.nature.com/leu)

bjh research paper

Regulation of angiogenesis in the bone marrow of myelodysplastic syndromes transforming to overt leukaemia

Tamara Keith,[1,2] Yuko Araki,[1] Masaki Ohyagi,[1] Maki Hasegawa,[1] Kouhei Yamamoto,[1] Morito Kurata,[1] Yasunori Nakagawa,[1,3] Kenshi Suzuki[3] and Masanobu Kitagawa[1]

[1]Department of Comprehensive Pathology, Aging and Developmental Sciences, Graduate School, Tokyo Medical and Dental University, Tokyo, Japan, [2]Department of Haematology, Imperial College, London, UK, and [3]Department of Hematology, Japanese Red Cross Medical Centre, Tokyo, Japan

Received 14 December 2006; accepted for publication 22 January 2007

Correspondence: Masanobu Kitagawa, MD, Department of Comprehensive Pathology, Aging and Developmental Sciences, Graduate School, Tokyo Medical and Dental University, 1-5-45 Yushima, Bunkyo-ku, Tokyo 113-8519, Japan. E-mail: masa.pth2@tmd.ac.jp

Summary

To investigate the regulatory mechanisms of angiogenesis in the development of myelodysplastic syndromes (MDS) and its progression to overt leukaemia (OL), bone marrow samples from control, paired samples from MDS patients before and after transformation to OL (MDS → OL) and *de novo* acute myeloid leukaemia (AML) were analysed. Immunohistochemical staining showed a significant increase of bone marrow microvascular density (MVD) in MDS and *de novo* AML compared with controls. Surprisingly, in MDS, MVD significantly decreased upon transformation to OL, which was also significantly lower than the MVD of *de novo* AML. This evidence was strengthened by the pattern of angiogenic mediator gene expression, confirming the importance of various angiogenic mediators including vascular endothelial growth factor (VEGF), basic fibroblast growth factor (bFGF), tumour necrosis factor α (TNFα), hepatocyte growth factor (HGF) and the angiopoietin family of mediators (Ang-1 and Ang-2) as well as the receptors for angiogenic mediators, such as VEGF receptor 2 (VEGFR2) and the tyrosine kinase receptor, TIE2. By contrast, the anti-angiogenic mediator, transforming growth factor-β (TGFβ) exhibited significantly higher expression in the bone marrow of MDS → OL, indicating the importance of this cytokine as the suppressive factor of angiogenesis in MDS. These findings indicate that the bone marrow microenvironment in MDS → OL and *de novo* AML differs remarkably, suggesting the different efficacy of anti-angiogenic therapy between *de novo* AML and leukaemia secondary to MDS.

Keywords: myelodysplastic syndromes, overt leukaemia, bone marrow, angiogenesis, microvasculature.

The myelodysplastic syndromes (MDS) are a heterogeneous group of clonal haemopoietic disorders, characterised by peripheral blood cytopenia of one or more lineages and, paradoxically in the majority of cases, a normocellular or hypercellular bone marrow, this finding being mainly caused by ineffective haemopoiesis (Mufti, 2004). The pathogenesis of MDS is a multi-step process, whereby a series of DNA mutations occur within a haemopoietic stem cell that adversely affect its differentiation and maturation, leading to aberrant cellular function including susceptibility to apoptosis. Tumour suppressor inactivation, telomere shortening and silencing of DNA mismatch repair genes increase genomic instability and cytogenetic abnormalities, contributing to disease progression and leukaemic transformation (Albitar *et al*, 2002; Mufti, 2004; Disperati *et al*, 2006).

Angiogenesis is the formation of new blood vessels from pre-existing vessels (Aguayo *et al*, 2000) and is understood to be involved in the growth, dissemination and metastasis of solid tumours (Folkman, 1971). A tumour up to 2 mm in size can absorb enough oxygen and nutrients by simple diffusion from the surrounding vasculature; however, a greater vascular network is required as the tumour grows (Moehler *et al*, 2003). Haematological malignancies do not develop in the same way as solid tumours so the requirement of angiogenesis for growth and development has not been as readily recognised as for other malignancies (Bertolini *et al*, 2000; Moehler *et al*, 2003).

However, Aguayo *et al* (2000) evaluated the importance of angiogenesis in leukaemia and MDS, and discovered increased vascularity, indicating that angiogenesis might have a role in the pathogenesis of haematological malignancies, initiating interest in this field.

Angiogenic growth factors include vascular endothelial growth factor (VEGF) (Orpana & Salven, 2002; Distler *et al*, 2003; Podar & Anderson, 2005), basic fibroblast growth factor (bFGF) (Moehler *et al*, 2003), tumour necrosis factor alpha (TNFα) (Stifter *et al*, 2005), tumour growth factor beta (TGFβ) (Distler *et al*, 2003), hepatocyte growth factor (HGF; thought to upregulate VEGF expression) (Van Belle *et al*, 1998; Bouis *et al*, 2006) and angiopoietin-1 (Ang-1) (Distler *et al*, 2003; Yu, 2005). VEGF and bFGF are the strongest inducers of angiogenesis (Albitar, 2001; Aguayo *et al*, 2003) and are synthesised in various types of cells (Moehler *et al*, 2003). The angiopoietins have both pro- and anti-angiogenic effects, acting via the tyrosine kinase receptor (TIE2). Ang-1, a pro-angiogenic factor causes autophosphorylation of TIE2 leading to endothelial cell sprouting and vessel stabilisation. Angiopoietin-2 (Ang-2) can act in opposite ways: it antagonises Ang-1, disrupting TIE2 activation and causing vessel destabilisation and regression; conversely, in the presence of VEGF, it facilitates endothelial cell proliferation (i.e. pro-angiogenic) (Distler *et al*, 2003; Tait & Jones, 2004). When there is an imbalance, angiogenesis is up- or downregulated in the mechanism described as the 'Angiogenic switch' (Lim & Levine, 2005). It is proposed that a larger vascular network provides an increased supply of oxygen and nutrients, facilitating the growth of the haematological clone and cells, such as osteoclasts, that produce pro-angiogenic factors, thus increasing angiogenesis further in a positive feedback circuit.

There is conflicting evidence regarding angiogenesis in MDS; some studies have proposed that bone marrow microvascular density (MVD) increases with MDS progression (Moehler *et al*, 2003; Wimazal *et al*, 2006), whereas others suggest increased vascularity in the early but not the latter stages of MDS (Campioni *et al*, 2004; Lundberg *et al*, 2006). Greater understanding of the role that angiogenesis plays in MDS will enable the development of therapies that can be targeted to the angiogenic pathway, thereby slowing disease progression and offering new hope to those patients for whom there are currently limited therapeutic options (Estey, 2004). The present investigation aimed to evaluate the changes in microvasculature and expression of angiogenic mediators during the development of MDS, and thus assess the role that angiogenesis plays in the progression of this disease.

Material and methods

Patients

Formalin-fixed paraffin-embedded bone marrow aspiration samples from 10 individuals with no morphological abnormalities were included as controls [mainly, patients with suspected idiopathic thrombocytopenic purpura (ITP) but with no morphological abnormality, male:female, 10 : 0; age, median 63 years (range 51–76 years)], 10 patients with MDS [three with refractory anaemia (RA), seven with RA with excess blasts (RAEB); male:female, 7:3; age, median 68 years (range, 48–77 years)] who developed overt leukaemia [OL, also classified as French–American–British (FAB) M2] later in the disease course (duration, 3 months to 3 years), and eight patients with *de novo* acute myeloid leukaemia (AML) [M2 according to the FAB classification, male:female, 4:4; age, median 60 years (range, 49–76 years)] were analysed. Age-matched control cases were included in order to exclude the influence of ageing on bone marrow cells. Diagnoses were based on standard clinical and laboratory criteria, including cell morphology (Bennett *et al*, 1982; Harris *et al*, 1999). All bone marrow aspirates were taken from the sternum and performed at the Japanese Red Cross Medical Centre, Tokyo, Japan. Control, MDS and *de novo* AML samples were collected at the time of the initial aspiration biopsy. The *de novo* AML samples exhibited a proliferation of blast cells accounting for >80% of all bone marrow cells. The patients were not infected with specific viruses, including human T cell leukaemia virus type 1 (HTLV-1), and had not been treated with therapeutic drugs prior to the study. After the initial diagnosis, MDS patients had received non-specific treatments, such as transfusion in case of severe anaemia and antibiotics or antipyretics when infectious symptoms appeared. However, they had not received any anti-cancer drugs even at the time of sample collection for OL. Bone marrow samples from MDS cases were also taken and analysed when the patients developed OL (MDS → OL). In addition, fresh frozen bone marrow samples from controls [nine cases, male:female, 4:5; age, median 62 (range, 44–87 years)], 10 paired MDS and MDS → OL patients and eight *de novo* AML cases described above were used for polymerase chain reaction (PCR) experiments.

The procedures were followed in accordance with the ethical standards established by the ethics committee of Tokyo Medical and Dental University.

Immunohistochemistry for measuring bone marrow MVD

Formalin-fixed tissue sections (10 μm) of bone marrow from controls (10 cases), MDS (10 cases) and *de novo* AML cases (eight cases) were prepared on slides covered with adhesive. Sections were deparaffinised, and endogenous peroxidase was quenched with 1·5% hydrogen peroxide in methanol for 10 min. Antibodies were applied to identify microvasculature. Primary antibodies included polyclonal rabbit antibody against von Willebrand factor (human vascular-associated antigens Factor VIII; Dako Cytomation, Glostrup, Denmark) and polyclonal rabbit antibody against VEGF receptor 2 (VEGFR2; Cell Signalling Technology, Tokyo, Japan). All sections were developed using biotin-conjugated secondary antibodies against rabbit IgG followed by a sensitive peroxidase-conjugated streptavidin system (Dako) with 3,3′ diaminobenzidine (DAB) as the chromogen. Negative control staining was

performed using rabbit immunoglobulin of irrelevant specificity substituted for the primary antibody.

The MVD was measured using methods described previously (Padro *et al*, 2000), systematically scanning the section to find the area of most intense vascularisation (hot spot), then counting the number of vessels and measuring vessel area at 20 × power objective lens, using the Leica Quantimet 600 high resolution image analysis system (Leica, Cambridge, UK). All the patients in the study were sampled at the time of initial diagnosis and at the time of OL development. One slide at a time was observed and the areas were measured in more than five fields per slide. The MVD was calculated using the equation: Relative vascular area (%) = (total area of blood vessels)/(total area examined) × 100.

Preparation of RNA and quantitative assay for angiogenic mediators using TaqMan reverse transcription polymerase chain reaction (RT-PCR)

RNA was extracted from frozen bone marrow samples of control subjects with no morphological abnormality, MDS patients with transformation to OL, and *de novo* AML patients using an RNeasy Mini Kit (Qiagen, Valencia, CA, USA) according to the manufacturer's directions. For quantitative RT-PCR, fluorescent hybridisation probes and the *Taq*Man PCR Core Reagents Kit with Ampli*Taq* Gold (PerkinElmer Cetus, Norwalk, CT, USA) were used with the ABI Prism 7900HT Sequence Detection System (PerkinElmer). Oligonucleotides (as specific primers) and *Taq*Man probes for the angiogenic mediators and glutaraldehyde-3-phosphate dehydrogenase (GAPDH) mRNA were synthesised at a commercial laboratory (PerkinElmer Cetus). The primers and *Taq*Man probes were as follows. The sequence of the forward primer for VEGF mRNA was 5′-GACC GCGACTCGGAGAGATG-3′ and that of the reverse primer, 5′-ATGTCCCTACTCCTGTGGCC-3′; the *Taq*Man probe was 5′-GGTCCAGTCTGCCTGTCTTTCTGTCTAGT-3′. For bFGF mRNA, the forward primer was 5′-GCCGTACATCGAGTACT AGATAC-3′ and the reverse primer, 5′-TCACTCGTTTAGAC GGGACG-3′; the *Taq*Man probe was 5′-ACAAAGATACA GCACCTTCGT-3′. For TNFα mRNA, the forward primer was 5′-GCTCAGACCCGTCCAGATGAAA-3′ and the reverse primer, 5′-AGGTTGGAAGGGTTTGCG-3′; the *Taq*Man probe was 5′-AGTAACGGGACACTCCTCCTGCTTGT-3′. The forward primer for HGF mRNA was 5′-CTCCGGTACCACGA-TATGAGAAC-3′ and the reverse primer, 5′-CGTTAATTTTGT ACGCGACTGT-3′; the *Taq*Man probe was 5′-GGGAGTGT GGGCGACCCTCATGACT-3′. The forward primer for TGFβ mRNA was 5′-GAGAGGCTGGACGGTGTCT-3′ and the reverse primer, 5′-TCTAGCGCGGGTAGATCCAA-3′; the *Taq*-Man probe was 5′-GGGATAAGTTCTGGTGGGTGGAAGA CCA-3′. The forward primer for Ang-1 mRNA was 5′-TCA CATAGGGTGCAGCAATCAG-3′ and the reverse primer, 5′-GT AGGCACATTGCCCATGTTG-3′; the *Taq*Man probe was 5′-CCGAAGTCCAGAAAACAGTGGGAGAAGATATA AC-3′. The forward primer for Ang-2 mRNA was 5′TTCCT CCTGCCAGAGATGGA-3′ and the reverse primer, 5′-TGCA-CAGCATTGGACACGTA-3′; the *Taq*Man probe was 5′-AA-CTGCCGCTCTTCCTCCAGCCC-3′. The forward primer for TIE2 mRNA was 5′-ACTTCGGTGCTACTTAACAACTTA-CATC-3′ and the reverse primer, 5′-CCTGGGCCTTGGTGTT-GAC-3′; the *Taq*Man probe was 5′-CAGGGAGCAGTA CGTGGTCCGAGCT-3′. The forward primer for VEGFR2 mRNA was 5′-CACCACTCAAACGCTGACATGTA-3′ and the reverse primer, 5′-CCAACTGCCAATACCAGTGGAT-3′; the *Taq*Man probe was 5′-TGCCATTCCTCCCCCGCATC-3′. The forward primer for glyceraldehyde-3-phosphate dehydrogenase (GAPDH) mRNA was 5′-GAAGGTGAAGGTCG-GAGT-3′ and the reverse primer, 5′-GAAGATGGTGATGG-GATTTC-3′; the *Taq*Man probe was 5′-CAAGCTTCCCG-TTCTCAGCC-3′. Conditions for the one-step RT-PCR were as follows: 30 min at 48°C (stage 1, reverse transcription), 10 min at 95°C (stage 2, RT inactivation and Ampli*Taq* Gold activation) and then 40 cycles of amplification for 15 s at 95°C and 1 min at 60°C (stage 3, PCR). The expression of angiogenic mediators was quantified according to a method described elsewhere (Yamamoto *et al*, 2004). Briefly, the intensity of the reaction was evaluated from the quantity of total RNA in HeLa cells (ng) corresponding to the initial number of PCR cycles to reveal the linear increase in reaction intensity (threshold cycle) for each sample on a logarithmic standard curve. Data on the quantity of RNA (ng) for angiogenic mediators were normalised using the data for GAPDH in each sample by the $2^{-\Delta\Delta CT}$ method (Livak & Schmittgen, 2001).

Double immunostaining for angiogenic mediators and cell marker

To examine the distribution of angiogenic mediator expressing cells in the bone marrow of MDS cases, mouse monoclonal antibody against VEGF (Santa Cruz Biotechnology Inc., Santa Cruz, CA, USA), polyclonal rabbit antibody against bFGF (Santa Cruz Biotechnology Inc.), mouse monoclonal antibody against TNFα (Serotec Ltd, Oxford, UK), or polyclonal rabbit antibody against TGFβ (Santa Cruz Biotechnology Inc.) were applied on 4 μm thick formalin-fixed tissue sections, after treatment with 0·3% hydrogen peroxide in methanol to delete endogenous peroxidase activity and 10% normal goat serum for blocking non-specific binding of the antibody. Sections were then incubated with goat anti-mouse or rabbit IgG antibody (Dako) followed by a sensitive peroxidase-conjugated streptavidin system (Dako) with DAB as the chromogen. Next, sections were treated with 0·1% trypsin in Tris buffer, 0·3% hydrogen peroxide in methanol, 10% normal goat serum, and then incubated with mouse monoclonal antibody for the macrophage-lineage cell marker anti-CD68 antibody (Dako). Sections were then incubated with goat anti-mouse IgG antibody followed by a sensitive peroxidase-conjugated streptavidin system with TrueBlue Peroxidase Substrate (KPL, Inc., Gaithersburg, MD, USA) as the chromogen.

Statistical analysis

Statistically significant differences in the quantitative analysis of MVD and mRNA expression were calculated using Mann–Whitney's *U*-test when comparing non-paired samples and Wilcoxon's test when comparing the paired samples, MDS and MDS → OL. Significant correlations between the collated data were calculated using Spearman's rank correlation coefficient. *P*-values < 0·05 were considered significant.

Results

Bone marrow MVD in controls, MDS, MDS → OL, and de novo AML cases

To allow MVD measurement, bone marrow specimens from nine controls, 10 paired MDS and MDS → OL, and eight *de novo* AML patients were immunostained for FVIII and VEGFR2. Distribution of FVIII and VEGFR2 antigens clearly visualised the vascular endothelium, which was easily distinguishable from megakaryocytes and enabled measurement of the MVD (Fig 1). The pattern of microvessels viewed with immunohistochemical staining for FVIII Fig 1A–D and VEGFR2 (Fig 1E and F) was consistent, regardless of which vascular-associated antigen was stained. The density of vessels was higher in MDS (Fig 1B) and *de novo* AML (Fig 1D and F) in contrast to the scarce staining in controls (Fig 1A) and MDS → OL (Fig 1C and E).

Statistical analysis of relative vascular area revealed significant differences among MVD of controls (median, 0·16; minimum–maximum, 0·01–0·24), MDS (0·22; 0·13–0·47), MDS → OL (0·07; 0·02–0·21) and *de novo* AML (0·39; 0·12–0·54) patients (Fig 2A). For simplicity, only the results of FVIII staining are shown because the results of VEGFR2 staining were almost the same as those of FVIII. Increased bone marrow vascularity was found in MDS ($P < 0·05$) and *de novo*

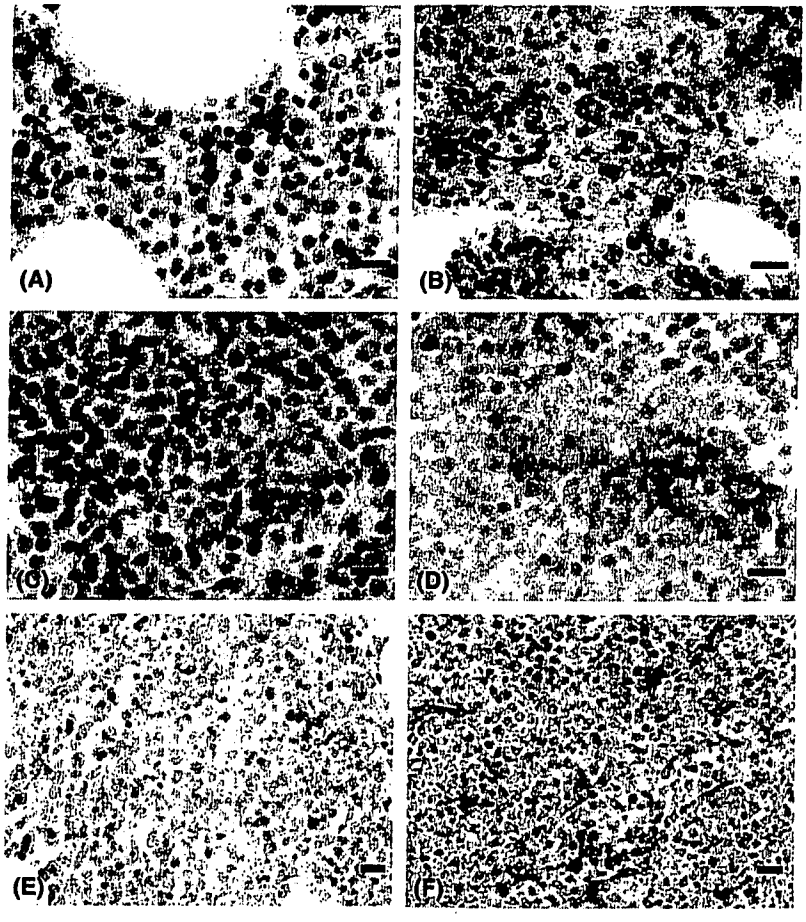

Fig 1. Immunohistochemical evaluation of vessels in the bone marrow of controls, MDS, MDS → OL, and *de novo* AML cases. Immunohistochemistry using anti-Factor VIII antigen identified blood vessels, clearly distinguishable from megakaryocytes (A, controls; B, MDS; C, MDS → OL; D, *de novo* AML; original magnification, 200×). Similarly, staining using anti-VEGFR2 clearly demonstrated higher density of blood vessels in *de novo* AML bone marrow (E) than that of MDS → OL bone marrow (F, original magnification, 100×). These images demonstrate the two antibodies produced staining of equal quality, identifying the vascular endothelium. Bars indicate 20 μm in each figure. Significant differences in vessel numbers were observed; controls and MDS → OL had the smallest amounts of vessels, *de novo* AML had numerous vessels; the numbers of vessels were intermediate in MDS.

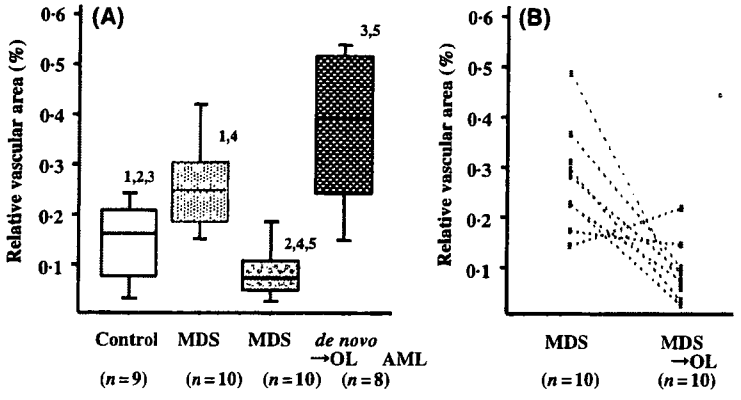

Fig 2. Comparison of the microvascular density (MVD) in the bone marrow of controls, MDS, MDS → OL, and *de novo* AML cases evaluated by image analysis using immunstaining for factor VIII antigen. (A) Box plot illustrating MVD measured, recorded as relative vascular area, in the bone marrow of controls, MDS, MDS → OL and *de novo* AML cases. Bars indicate 90% tile and 10% tile and boxes indicate 75% tile to 25% tile with lines of median values inside the boxes. Differences were significant between the MVD of controls and MDS ($^1P < 0{\cdot}01$), controls and MDS → OL ($^2P < 0{\cdot}05$), controls and *de novo* AML ($^3P < 0{\cdot}05$), MDS and MDS → OL ($^4P < 0{\cdot}001$), and MDS → OL and *de novo* AML ($^5P < 0{\cdot}01$). (B) Paired comparisons of the bone marrow MVD of patients with MDS and after transformation to OL. MVD was measured from paired bone marrow samples of patients with MDS and after transformation to OL. Note the decline in relative vascular area between MDS and MDS → OL, which was statistically significant ($P < 0{\cdot}05$).

Table I. Quantitative analysis of angiogenic mediators in the bone marrow of controls, MDS, MDS → OL, and *de novo* AML cases determined by RT-PCR (the quantity of mRNA for angiogenic mediators normalised to that of GAPDH).

Mediator	Controls (n = 9)	MDS (n = 10)	MDS → OL (n = 10)	*de novo* AML (n = 8)
VEGF	0·66* (0·10–0·85)	0·54 (0·29–4·20)	0·73 (0·20–4·45)	1·13 (0·13–4·49)
bFGF	0·02 (0. 01–0·15)	0·09 (0·03–3·30)	0·04 (0·01–8·76)	0·64 (0·04–9·48)
TNFα	0·06 (0. 01–0·26)	0·24 (0·05–3·88)	0·11 (0·07–2·20)	1·95 (0·02–3·00)
HGF	0·05 (0. 01–0·21)	0·33 (0·06–4·59)	0·17 (0·04–3·25)	0·67 (0·06–62·9)
Ang-1	0·01 (0. 0002–0·09)	0·16 (0·02–3·27)	0·13 (0·01–2·51)	0·65 (0·01–6·41)
Ang-2	0·01 (0. 0004–0·25)	0·20 (0·03–4·42)	0·20 (0·03–2·84)	0·85 (0·02–20·8)
TGFβ	1·40 (0·14–6·62)	2·64 (1·00–12·4)	5·46 (1·03–25·2)	2·85 (0·16–62·9)
VEGFR2	0·14 (0·09–0·85)	0·15 (0·03–4·57)	0·10 (0·04–1·54)	0·28 (0·01–14·2)
TIE2	0·09 (0. 04–1·50)	0·15 (0·03–2·68)	0·10 (0·02–1·40)	0·42 (0·01–17·1)

*Values indicated are the median (range).

AML ($P < 0{\cdot}05$) patients when compared with controls. Overall, MDS patients exhibited significantly lower MVD after transformation to OL ($P < 0{\cdot}05$) and MDS → OL had lower MVD than *de novo* AML ($P < 0{\cdot}01$). Median MVD values were higher in *de novo* AML than MDS, although the difference was not statistically significant. No significant difference was demonstrated between controls and MDS → OL. Pairwise comparison of MDS and MDS → OL samples clearly showed a significant reduction of MVD in MDS after transformation to OL (Fig 2B). As shown, nine of 10 MDS patients showed reduced MVD when OL developed. The remaining case showed a very small increase of MVD.

Quantitative analysis of the expression of mRNA for angiogenic mediators

To determine the gene expression intensity of angiogenic mediators VEGF, bFGF, TNFα, HGF, Ang-1, Ang-2 and TGFβ in the bone marrow specimens of controls, MDS, MDS → OL and *de novo* AML cases, real-time quantitative RT-PCR was performed (Table I). As shown in Fig 3A, VEGF expression was greater in *de novo* AML compared with controls ($P < 0{\cdot}001$) and MDS ($P < 0{\cdot}001$) but no other significant differences were found when comparing patient groups. The pro-angiogenic factors bFGF (Fig 3B), TNFα (Fig 3C), HGF (Fig 3D), and Ang-1 (Fig 3E) had significantly higher expression in MDS and *de novo* AML compared to controls, with higher expression in *de novo* AML compared with MDS. The gene expression of bFGF, TNFα and HGF was significantly higher in MDS patients prior to transformation to OL, and gene expression of bFGF in MDS → OL was significantly lower than that of *de novo* AML. The median value of gene expression of these factors was consistently greater in MDS → OL than controls, although this was not statistically significant.

To investigate whether the anti-angiogenic factors play a role in MVD, mRNA expression for Ang-2 and TGFβ was determined. As shown in Fig 3F, the expression pattern of Ang-2 in controls, MDS, MDS → OL and *de novo* AML was

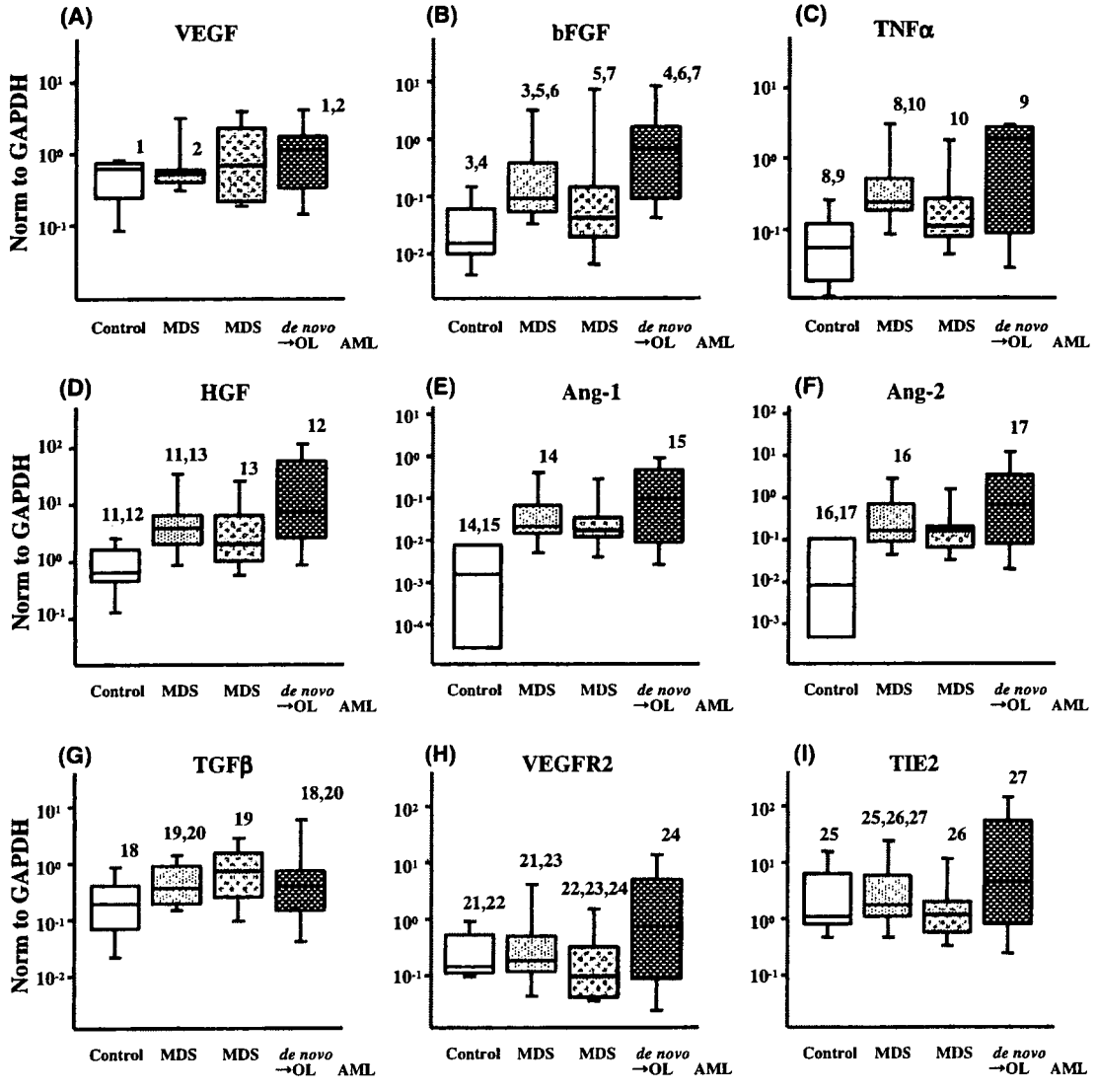

Fig 3. Expression of angiogenic mediators in the bone marrow of controls, MDS, MDS → OL, and *de novo* AML cases, as determined by RT-PCR. These box plots compare the levels of mRNA expression for VEGF (A), bFGF (B), TNFα (C), HGF (D), Ang-1 (E), Ang-2 (F), TGFβ (G) gene expression between controls, MDS, MDS → OL and *de novo* AML cases. Similarly, expression levels of receptors for angiogenic mediators, VEGFR2 (H) and TIE2 (I) were compared between controls, MDS, MDS → OL and *de novo* AML cases. Bars indicate 90% tile and 10% tile and boxes indicate 75% tile to 25% tile with lines of median values inside the boxes. Differences were significant between the expression levels in controls and *de novo* AML ($^1P < 0{\cdot}001$), and MDS and *de novo* AML ($^2P < 0{\cdot}001$) of VEGF, controls and MDS ($^3P < 0{\cdot}001$), controls and *de novo* AML ($^4P < 0{\cdot}01$), MDS and MDS → OL ($^5P < 0{\cdot}01$), MDS and *de novo* AML ($^6P < 0{\cdot}001$), and MDS → OL and *de novo* AML ($^7P < 0{\cdot}05$) of bFGF, controls and MDS ($^8P < 0{\cdot}05$), controls and *de novo* AML ($^9P < 0{\cdot}05$), and MDS and MDS → OL ($^{10}P < 0{\cdot}01$) of TNFα, controls and MDS ($^{11}P < 0{\cdot}01$), controls and *de novo* AML ($^{12}P < 0{\cdot}01$), and MDS and MDS → OL ($^{13}P < 0{\cdot}05$) of HGF, controls and MDS ($^{14}P < 0{\cdot}01$), and controls and *de novo* AML ($^{15}P < 0{\cdot}05$) of Ang-1, controls and MDS ($^{16}P < 0{\cdot}05$), and controls and *de novo* AML ($^{17}P < 0{\cdot}05$) of Ang-2, controls and *de novo* AML ($^{18}P < 0{\cdot}001$), MDS and MDS → OL ($^{19}P < 0{\cdot}01$), and MDS and *de novo* AML ($^{20}P < 0{\cdot}001$) of TGFβ. Expression levels of receptors for angiogenic mediators exhibited significant differences between controls and MDS ($^{21}P < 0{\cdot}001$), controls and MDS → OL ($^{22}P < 0{\cdot}001$), MDS and MDS → OL ($^{23}P < 0{\cdot}001$), MDS → OL and *de novo* AML ($^{24}P < 0{\cdot}001$) of VEGFR2, controls and MDS ($^{25}P < 0{\cdot}001$), MDS and MDS → OL ($^{26}P < 0{\cdot}01$), and MDS and *de novo* AML ($^{27}P < 0{\cdot}001$) of TIE2.

quite similar to that of Ang-1. TGFβ expression was in contrast to that of the pro-angiogenic factors, having significantly higher expression after transformation to OL than in MDS ($P < 0{\cdot}01$), although, like the other pro-angiogenic factors, TGFβ showed increased expression in *de novo* AML compared with controls ($P < 0{\cdot}001$) (Fig 3G).

Quantitative analysis of the expression of mRNA for receptors to angiogenic mediators

As shown in Fig 3H, VEGFR2 expression followed the trend of the other pro-angiogenic factors, with greatest expression in *de novo* AML, and higher expression in MDS compared with

Table II. Correlations between MVD and expression intensities of angiogenic mediators.

	MVD	VEGF	bFGF	TNFα	HGF	Ang-1	Ang-2	TGFβ	VEGFR2	TIE2
MVD		NS	<0·05	<0·05	0·051	0·06	0·08	NS	<0·05	<0·05
VEGF	NS		<0·05	<0·05	NS	<0·05	<0·05	NS	0·055	<0·05
bFGF	<0·05	<0·05		<0·01	<0·05	<0·01	<0·01	NS	<0·05	<0·01
TNFα	<0·05	<0·05	<0·01		<0·05	<0·01	<0·01	NS	<0·05	<0·01
HGF	0·051	NS	<0·05	<0·05		<0·05	<0·05	NS	NS	<0·05
Ang-1	0·06	<0·05	<0·01	<0·01	<0·05		<0·001	NS	NS	<0·01
Ang-2	0·08	<0·05	<0·01	<0·01	<0·05	<0·001		NS	NS	<0·01
TGFβ	NS	NS	NS	NS	NS	NS	NS		NS	NS
VEGFR2	<0·05	0·055	<0·05	<0·05	NS	NS	NS	NS		<0·05
TIE2	<0·05	<0·05	<0·01	<0·01	<0·05	<0·01	<0·01	NS	<0·05	

*Values indicate the *P*-value calculated using Spearman's rank correlation coefficient. NS, not significant.

controls ($P < 0·001$) and MDS → OL ($P < 0·001$). Bone marrow samples from MDS → OL showed significantly lower VEGFR2 expression compared with those from *de novo* AML, MDS and controls ($P < 0·001$). Similarly, TIE2 expression showed significant differences between controls and MDS ($P < 0·001$), MDS and MDS → OL ($P < 0·01$), and MDS and *de novo* AML ($P < 0·001$) (Fig 3I).

Correlation of MVD and mRNA expression for angiogenic mediators and receptors

The immunohistochemical and PCR results identified a strong correlation between MVD and the expression of the receptors for pro-angiogenic mediators, VEGFR2 and TIE2 ($P < 0·05$) (Table II). Gene expression of TNFα and bFGF also correlated with MVD ($P < 0·05$). The expression of pro-angiogenic factors, VEGF, TNFα, HGF, bFGF, Ang-1 and Ang-2 showed strong correlation with one another (data not shown). The most significant correlations were observed between the expression of Ang-1 and Ang-2 ($P < 0·001$) and Ang-1 and Ang-2 with receptor TIE2 ($P < 0·01$). Expression of bFGF correlated with the expression of all pro-angiogenic factors ($P < 0·01$ or $P < 0·05$) and reversely correlated with TGFβ expression ($P < 0·05$). TNFα showed strong correlations with bFGF, Ang-1, Ang-2 and TIE2 expression ($P < 0·01$ or $P < 0·05$). HGF showed no correlation with VEGF but correlated with the other pro-angiogenic factors ($P < 0·05$). Interestingly expression of the receptors, TIE2 and VEGFR2, correlated ($P < 0·05$). These results suggest the presence of an autocrine circuit influencing angiogenesis.

Localisation of angiogenic mediator producing cells in the bone marrow of MDS cases

The bone marrow environment is regulated by stromal cells, including endothelial cells and macrophage-lineage cells. Macrophage-lineage cells play a very crucial role in regulating haematopoiesis in MDS bone marrow (Kitagawa *et al*, 1997). To determine whether the cells expressing angiogenic mediators in MDS bone marrow were macrophage-lineage or not, double immunostaining for cell marker, CD68 and angiogenic mediators was performed. As shown in Fig 4, VEGF (A) and TGFβ (G) antigens were localised to CD68-negative cells, indicating that these molecules were mainly produced by haematopoietic cells in MDS bone marrow. By contrast, bFGF (C) and TNFα (E) were localised to CD68-positive macrophage-lineage cells, although bFGF was also localised to CD68-negative cells. When OL developed, some CD68-negative haematopoietic cells remained positive for VEGF antigen (B). However, angiogenic mediators, such as bFGF (D) and TNFα (F) positive cells, reduced in number, while TGFβ antigen was expressed in the blasts of OL bone marrow (H).

Discussion

The present study demonstrated a significant increase of MVD in *de novo* AML patients compared with controls, as previously demonstrated (Padro *et al*, 2000). The MVD in MDS was higher than in controls but lower than found in *de novo* AML and confirmed the results of Pruneri *et al* (1999), who proposed this implied angiogenesis was linked to the progression of MDS to OL. However, the present study clearly showed a decline in MVD upon transformation to OL from MDS, and showed that the MVD of MDS → OL was significantly lower than that of *de novo* AML. Gene expression of the angiogenic mediators also highlighted significant differences between MDS → OL and *de novo* AML, showing that, like MDS, *de novo* AML had higher expression of pro-angiogenic factors than MDS → OL.

Morphologically, blasts in MDS → OL and *de novo* AML patients were very similar; both groups are classified as FAB type AML M2, however, significantly different angiogenic activity has been demonstrated between the two groups. These findings indicate that the bone marrow microenvironment, and thus pathogenic events, in these diseases differs, as the clinical features, karyotypic abnormalities and responses to chemotherapy are different. The transformation of MDS to OL would be a multi-step, complex process. Our evidence suggests

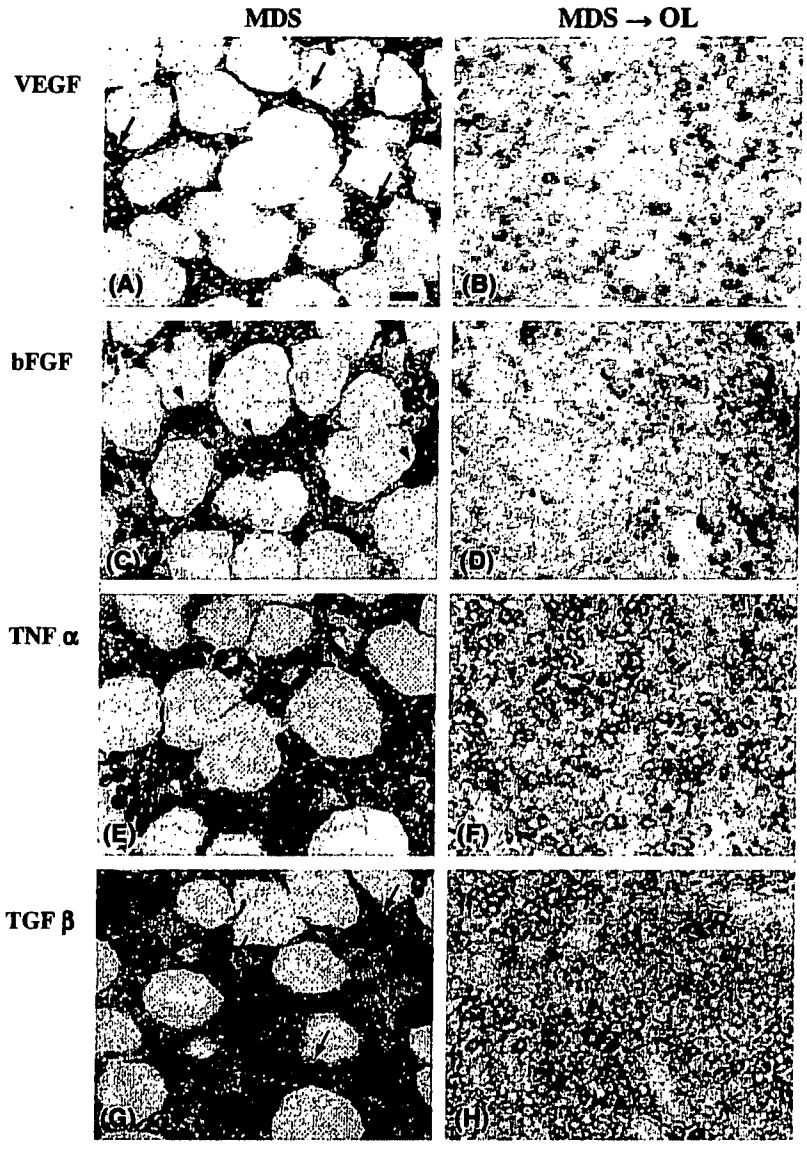

Fig 4. Immunohistochemical localisation of VEGF (A,B), bFGF (C,D), TNFα (E,F), and TGFβ (G,H) in the bone marrow of MDS cases at the time of initial diagnosis (MDS) and after evolution of OL (MDS → OL) (same magnification). Double immunostains for each mediator and the macrophage-lineage cell marker, CD68 in the bone marrow of MDS (A,C,E,G) and MDS → OL (B,D,F,H) are shown. Double immunostaining revealed positive reactions for each angiogenic mediator (brown) and the cell marker (blue). The bar in (A) indicates 20 μm. Note that VEGF- or TGFβ-positive cells in MDS bone marrow were CD68-negative (A and G, arrows), while bFGF or TNFα positive cells were also positive for CD68 antigen (C and E, arrowheads), although some bFGF positive cells were CD68-negative.

that, like *de novo* AML, MDS has increased angiogenesis; however, MDS → OL appears not to be as dependent upon angiogenesis as *de novo* AML, so there must be a point in the transformation of MDS to OL where disease evolution becomes independent of angiogenesis or resistant to angiogenic factors and no longer requires increased vascularity for increased proliferation and clonal expansion. This might be related to the chemotherapy-resistant nature of blasts in MDS → OL. Furthermore, reduced MVD could be an obstacle to the delivery of therapeutic drugs to the bone marrow environment. We suggest that anti-angiogenic drugs, i.e. targeted molecular therapy, would display differing efficacy between *de novo* AML and leukaemia secondary to MDS.

Angiogenic growth factors include VEGF, bFGF, TNFα, TGFβ and HGF. VEGF and bFGF are the strongest inducers of angiogenesis, synthesised in leukaemic and myeloma cells as well as fibroblasts, immune cells, osteoclasts, thrombocytes and megakaryocytes (Moehler *et al*, 2003). Aguayo *et al* (2000) demonstrated increased serum levels of VEGF, bFGF and HGF in *de novo* AML and MDS, and their association with increased MVD. The present study also showed that the gene expression of these factors was upregulated in the bone

